

Analysis of a competitive respiratory disease system with quarantine*

Anna Daniel Fome^{†‡}, Wolfgang Bock[†], and Axel Klar[†]

Abstract. In the world of epidemics, the mathematical modeling of disease co-infection is gaining importance due to its contributions to mathematics and public health. Because the co-infection may have a double burden on families, countries, and the universe, understanding its dynamics is paramount. We study a SEIQR (susceptible-exposed-infectious-quarantined-recovered) deterministic epidemic model with a single host population and multiple strains ($-c$ and $-i$) to account for two competitive diseases with quarantine effects. To model the role of quarantine and isolation efficacy in disease dynamics, we utilize a linear function. Further, we shed light on the standard endemic threshold and determine the conditions for extinction or coexistence with and without forming co-infection. Next, we show the dependence of the criticality based on specific parameters of the different pathogens. We found that the disease-free equilibrium (DFE) of the single-strain model always exists and is globally asymptotically stable (GAS) if $\tilde{\mathcal{R}}_k^q \leq 1$, else, a stable endemic equilibrium. On top of that, the model has forward bifurcation at $\tilde{\mathcal{R}}_k^q = 1$. In the case of a two-strain model, the strain with a large reproduction number outcompetes the one with a smaller reproduction number. Further, if the co-infected quarantine reproduction number is less than one, the infections of already infected individuals will die out, and co-infection will persist in the population otherwise. We note that the quarantine and isolation of exposed and infected individuals will reduce the number of secondary cases below one, consequently reducing the disease complications if the total number of people in the quarantine is at most the critical value.

Key words. Respiratory disease, competition, co-existence, co-infection, quarantine efficacy, and equilibria states.

1. Introduction. An acute respiratory disease (ARI) is amongst the five respiratory conditions responsible for the tremendous burden to the society [27], particularly in low- and middle-income countries [13, 33]. It is a condition caused by an infectious agent, viruses, or mixed viral-bacterial infections that disturb body organs and the airway system. Some of the pathogens that cause this condition include influenza virus as well as severe acute respiratory syndrome coronavirus (SARS CoV) [33] of which they are responsible for several pandemics and emergencies of global consideration; for example, the most severe flu pandemic known as *Spanish flu* which occurred in 1918. The outbreak took approximately 50 million lives and infected half of the globe's population [22].

Since 1918, the human worries and great suffering of individuals, families, and communities changed the world's impression of flu-like illness [22]. In recent years, the emergence of severe acute respiratory syndrome coronavirus 2 (SARS-CoV-2) has demonstrated beyond doubt its ability to infect humans and cause widespread outbreaks. The virus originated in Wuhan City, China, at the beginning of December 2019 (henceforth Covid-19). A few months later (On March 11, 2020), the World Health Organization (WHO) declared Covid-19 as a global outbreak of pandemic[20].

The increased number of reported infections and deaths due to the flu-like pandemic inspired many researchers to investigate the co-exists of multiple illnesses. Several clinical studies on the subject are particularly relevant [5, 14, 23, 24, 25, 38, 40, 45]. To manage coexistence, distinguishing the two conditions from each other is necessary. However, due to similar clinical features of the existing diseases, identifying the etiologic agent through laboratory testing is recommended [24]. Moreover, as flu-like infections (in particular coronavirus and influenza) prompt severe complications and high mortality in a population, the co-infections suggest the consideration of comorbidity [5].

Furthermore, bio-mathematicians and medical experts are considerable regarding acute disease management [2] to understand the dynamics of some co-infection regardless of the novelty of the disease and the complexity of the profound etiology. The assimilation of these interactions through mathematical models to inform the population regarding the disease condition and the uncertainty linked with the infection have been studied [1, 8, 17, 21, 26, 32, 35, 36, 39] and the references therein. Based on control measures: mathematical modeling studies have depicted a positive impact upon applying quarantine during the disease outbreak [3, 6, 7, 12]

thirteen compartments: the individuals who are vulnerable to getting a disease upon contact with infectious denoted by S ; the exposed individuals are E_i , E_c , and E_{ic} ; individuals who are capable spreading the disease are I_i , I_c , and I_{ic} ; the classes Q_i , Q_c , and Q_{ic} are the individuals quarantined or detached; as well as R_i , R_c , and R_{ic} , the recovered individuals.

2.1. Main assumption statements.

1. **Vital dynamics:** In 1989, in his literature [19], Hethcote argued the fact of including inflow (birth) and outflow (death) when modeling the disease persisted in a population; so we assumed our model to reflect such kind of diseases.
2. **Formation of co-infected class:** If an individual carries two or more pathogens, that person is co-infected. Therefore, we assume that when a symptomatic individual with pathogen i gets in contact with another individual infected with pathogen c , or vice-versa the co-exposed class E_{ic} formed. On the contrary, co-existence is the state or fact of both strains existing in the same population at time t .
3. **Quarantine and Isolation:** We assumed that quarantined individuals are either recognized as a recent contact with a confirmed case or symptomatic. We have ignored the quarantine of the healthy population. To be clear and specific, we define an imperfect quarantine: as any quarantine site or facility (including home) characterized by violating any guidelines, rules, and regulations to control the spread of infections. For instance
 - (a) *Home quarantine:* an individual may want to go out for several reasons, like shopping or getting fresh air before quarantine maturity time. In such a case, if the individual is carrying the disease can transmit the virus (however, at a reduced rate).
 - (b) *Campsite quarantine:* In this case, an exposed individual (not carrying the virus) may become infected in the campsite due to the movements or activities when the quarantine rules are violated.

We employ a linear function (2.1) studied by [16, 29] to portray a reduction of disease transmission because of introducing control measures. We used the parameter ω_k to measure the potential inputs provided by the respective authority and assume it is proportional to the number of infected individuals. The inputs include but are not limited to biomedical waste management, provision of medical equipment, social and psychosocial support, and protections, as well as support to meet their basic needs. Moreover, education about infection preventive measures and the importance of promptly seeking medical care if they develop symptoms [34]. We let $\Omega_k(I_k) = \Omega_k$ be a continuously differentiable function w.r.t. to I_k defined as

$$(2.1) \quad \Omega_k = 1 - \omega_k I_k = \begin{cases} 0, & \text{if } I_k \omega_k = 1, \\ (0, 1], & \text{if } I_k \omega_k \in [0, 1), \end{cases}$$

where k stands for subscript i, c, ic . For all $I_k \in (0, 1)$ we assume $\omega_k \in [0, 1]$ (hence $\Omega_k \notin \mathbb{R}^-$). As an approximation to function (2.1), $\omega_k I_k$ and Ω_k satisfies the following as ω_k and I_k varies:

Perfect quarantine: Note, we assumed that, ω_k is proportional to I_k : hence as $I_k \rightarrow 1$, also $\omega_k \rightarrow 1$, and $I_k\omega_k \rightarrow 1$. For perfect quarantine, we hold that $I_k\omega_k \approx 1$ so, $\Omega_k = 0$.

Imperfect quarantine: In this case, for all $I_k \in (0, 1)$ and $\omega_k \in (0, 1]$ we have the following estimates:

Changes in		Level of imperfection
ω_k, I_k	$\omega_k I_k, \Omega_k$	
$\omega_k \rightarrow 0, I_k \rightarrow 0$	$\omega_k I_k \rightarrow 0, \Omega_k \rightarrow 1$	high
$\omega_k \rightarrow 0, I_k \rightarrow 1$	$\omega_k I_k \rightarrow 0, \Omega_k \rightarrow 1$	high
$\omega_k \rightarrow 1, I_k \rightarrow 0$	$\omega_k I_k \rightarrow 0, \Omega_k \rightarrow 1$	high
$\omega_k \rightarrow 1, I_k \rightarrow 1$	$\omega_k I_k \rightarrow 1, \Omega_k \rightarrow 0$	low

Table 1

Estimated level of imperfection

From equation (2.1) and Table 1, one can observe that "the smaller the value of Ω_k is, the effective quarantine is; in other words, as the value of Ω_k approaches zero, the smaller the chance of quarantined individuals to be infected.

4. **Cross-immunity:** A recent study by Almazán and her colleagues [4] investigated how influenza's pre-existing immunity to SARS-CoV-2 predicts Covid-19 dynamics. The study identified eleven CD8 T-cell peptides cross-reacted with flu and SARS-CoV-2 pathogens depending on the leukocyte antigen type. The detailed mathematical model of cross-immunity is given briefly in the book by Martcheva [28] and detailed further in [10, 31]. Thus, with parameters $\eta_i, \eta_c \in [0, 1]$, we model the immune response for individuals who have recovered from *pathogen i* to be sick with *pathgen c* or contrariwise. The values $\eta_i = 0$ and $\eta_c = 0$ correspond to full cross-immunity, and $\eta_i = 1$ and $\eta_c = 1$ equals no cross-immunity. We further assume that an individual who recovered from one strain has permanent immunity to that strain.

2.2. Model formulation. We assumed that all individuals are recruited into the susceptible population S with a constant inflow rate Λ and decrease by the rate μ , natural death from each class. The susceptible individuals become infected via contact with an infectious individual and move into the exposed class E_i or E_c . At the rates ρ_i and ρ_c the portions of E_i and E_c will progress to the infectious classes I_i and I_c , respectively. The progression of co-exposed individuals to active co-infections occurs at the rate ρ_{ic} . With the rates α_i, α_c and α_{ic} the exposed individual will enter the Q_i, Q_c , and Q_{ic} classes and further to I_i, I_c , and I_{ic} at the rates τ_i, τ_c and τ_{ic} , respectively. The growth in the quarantine from the infectious classes is at the rates σ_i, σ_c , and σ_{ic} . The fractions of infected and quarantine classes will progress to the recovered classes at the recovery rates γ and ϕ comparable to the number of people in their compartment. We summarize subsection 2.1, and subsection 2.2 in Figure 1. From the figure, ξ_i and ξ_c define strain- i and strain- c forces of infections, respectively, are given by

$$(2.2) \quad \xi_i = \frac{\beta_i(I_i + I_{ic} + \Omega_i Q_i + \Omega_{ic} Q_{ic})}{N_T}, \quad \text{and} \quad \xi_c = \frac{\beta_c(I_c + I_{ic} + \Omega_c Q_c + \Omega_{ic} Q_{ic})}{N_T}.$$

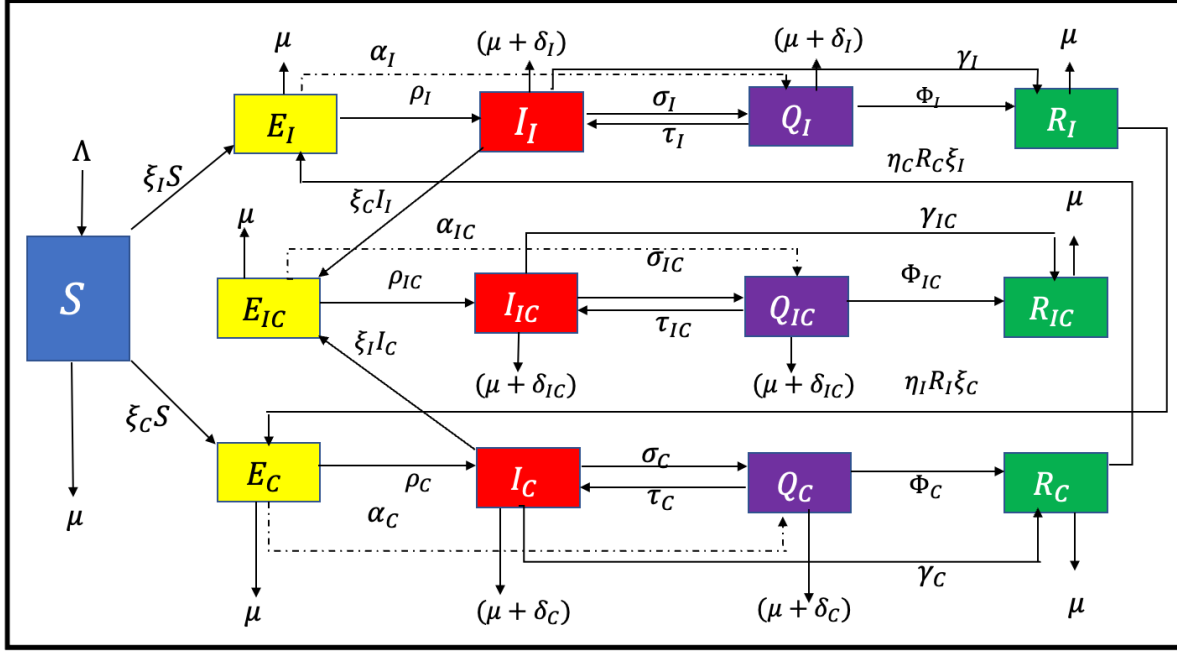


Figure 1. Two-strain epidemic with cross-immunity and co-infection

In (2.2), β_i and β_c are the contact rates where Ω_i , Ω_c and Ω_{ic} are the decreasing functions of infectiousness given in (2.1). Using the above assumptions, Figure 1, and parameters descriptions in Table 2, the following system equations are obtained:

$$\begin{aligned}
 (2.3) \quad & S'(t) = \Lambda - \xi_i S - \xi_c S - \mu S, \\
 & E'_i(t) = \xi_i S + \eta_c R_c \xi_i - \mathbf{p}_i E_i, \\
 & E'_c(t) = \xi_c S + \eta_i R_i \xi_c - \mathbf{p}_c E_c, \\
 & E'_{ic}(t) = \xi_i I_c + \xi_c I_i - \mathbf{p}_{ic} E_{ic}, \\
 & I'_i(t) = \rho_i E_i + \tau_i Q_i - \xi_c I_i - \mathbf{q}_i I_i, \\
 & I'_c(t) = \rho_c E_c + \tau_c Q_c - \xi_i I_c - \mathbf{q}_c I_c, \\
 & I'_{ic}(t) = \rho_{ic} E_{ic} + \tau_{ic} Q_{ic} - \mathbf{q}_{ic} I_{ic}, \\
 & Q'_i(t) = \alpha_i E_i - \mathbf{r}_i Q_i + \sigma_i I_i, \\
 & Q'_c(t) = \alpha_c E_c - \mathbf{r}_c Q_c + \sigma_c I_c, \\
 & Q'_{ic}(t) = \alpha_{ic} E_{ic} - \mathbf{r}_{ic} Q_{ic} + \sigma_{ic} I_{ic}, \\
 & R'_i(t) = \phi_i Q_i + \gamma_i I_i - \eta_i R_i \xi_c - \mu R_i, \\
 & R'_c(t) = \phi_c Q_c + \gamma_c I_c - \eta_c R_c \xi_i - \mu R_c, \\
 & R'_{ic}(t) = \phi_{ic} Q_{ic} + \gamma_{ic} I_{ic} - \mu R_{ic},
 \end{aligned}$$

where

$$\begin{aligned} \mathbf{p}_i &= \alpha_i + \rho_i + \mu, & \mathbf{p}_c &= \alpha_c + \rho_c + \mu, & \mathbf{p}_{ic} &= \alpha_{ic} + \rho_{ic} + \mu, \\ \mathbf{q}_i &= \gamma_i + \sigma_i + \delta_i + \mu, & \mathbf{q}_c &= \gamma_c + \sigma_c + \delta_c + \mu, & \mathbf{q}_{ic} &= \gamma_{ic} + \sigma_{ic} + \delta_{ic} + \mu, \\ \mathbf{r}_i &= \phi_i + \tau_i + \delta_i + \mu, & \mathbf{r}_c &= \phi_c + \tau_c + \delta_c + \mu, & \mathbf{r}_{ic} &= \phi_{ic} + \tau_{ic} + \delta_{ic} + \mu. \end{aligned}$$

At a given time t , the total population size N_T is given by

$$\begin{aligned} N_T(t) &= S(t) + E_i(t) + E_c(t) + E_{ic}(t) + I_i(t) + I_c(t) + I_{ic}(t) \\ &\quad + Q_i(t) + Q_c(t) + Q_{ic}(t) + R_i(t) + R_c(t) + R_{ic}(t). \end{aligned}$$

Moreover, the system (2.3) is equipped with strictly non-negative initial data

$$(2.4) \quad \begin{aligned} S(0) &\geq 0, \quad E_i(0) \geq 0, \quad E_c(0) \geq 0, \quad E_{ic}(0) \geq 0, \\ I_i(0) &\geq 0, \quad I_c(0) \geq 0, \quad I_{ic}(0) \geq 0, \quad Q_i(0) \geq 0, \quad Q_c(0) \geq 0, \\ Q_{ic}(0) &\geq 0, \quad R_i(0) \geq 0, \quad R_c(0) \geq 0, \quad \text{and} \quad R_{ic}(0) \geq 0. \end{aligned}$$

2.3. Basic Properties of the main model. Because we are dealing with problems related to population dynamics, for meaningful biological interpretation, all the variables must be positive and bounded for all time $t \geq 0$. Proofs are in the [Appendix A](#).

3. Results and discussion.

3.1. Analysis of Single-Strain model-SSM. Before analyzing the entire model, it is significant to investigate the dynamics of the single-strain model (SSM), this means that either strain- c or strain- i is absent. To generalize, we ask I_k to be some infected individuals with strain- i or strain- c . Here, we assume that the subscript k stands for either i or c . To this extent, the reduced imperfect model (i.e., $\Omega_k \in (0, 1]$) has eight equations less than model (2.3):

$$(3.1) \quad \begin{aligned} S'(t) &= \Lambda - \xi_k S - \mu S, \\ E'_k(t) &= \xi_k S - \mathbf{p}_k E_k, \\ I'_k(t) &= \rho_k E_k + \tau_k Q_k - \mathbf{q}_k I_k \\ Q'_k(t) &= \alpha_k E_k - \mathbf{r}_k Q_k + \sigma_k I_k, \\ R'_k(t) &= \phi_k Q_k + \gamma_k I_k - \mu R_k, \end{aligned}$$

where the force of infection and the total population size of the reduced model are correspondingly given by

$$(3.2) \quad \xi_k = \frac{\beta_k(I_k + \Omega_k Q_k)}{N_k}, \quad \text{and}, \quad N'_k(t) = \Lambda - \mu N_k - \delta_k(I_k + Q_k).$$

We suspend the proofs of positivity and boundness of the solutions in [Appendix A.3](#).

Symbol	Intepretation	Range/Value	Source
Λ	Recruitment rate	[0.001, 0.1]	Assumed
β_i	strain- i transmission rate	[0.5, 2]	[31]
β_c	strain- c transmission rate	[0.5, 2]	[6, 15]
ω_i	The parameter to measure the potential input in Q_i	[0, 1]	Assumed
ω_c	The parameter to measure the potential input in Q_c	[0, 1]	Assumed
ω_{ic}	The parameter to measure the potential input in Q_{ic}	[0, 1]	Assumed
Ω_i	Function to reduce the infection and measure the Q_i efficacy	[0, 1]	[6]
Ω_c	Function to reduce the infection and measure the Q_c efficacy	[0, 1]	[6]
Ω_{ic}	Function to reduce the infection and measure the Q_{ic} efficacy	[0, 1]	[6]
ρ_i	Rate of developing strain- i symptoms	[1/14,1/3]	[15]
ρ_c	Rate of developing strain- c symptoms	[1/14,1/3]	[15]
ρ_{ic}	Rate of developing co-infections symptoms	[1/14,1/3]	Assumed
α_i	Quarantine rate for strain- i exposed individuals	[0,2]	Assumed
α_c	Quarantine rate for strain- c exposed individuals	[0,2]	Assumed
α_{ic}	Quarantine rate for co-exposed individuals	[0,2]	Assumed
σ_i	Isolation rate for strain- i infected individuals	[0,2]	Assumed
σ_c	Isolation rate for strain- c infected individuals	[0,2]	Assumed
σ_{ic}	Isolation rate for co-infected individuals	[0,2]	Assumed
τ_i	Rate of strain- i quarantine-exposed individuals become I_i	$\rho_i \times 0.15$	Assumed
τ_c	Rate of strain- c quarantine-exposed individuals become I_c	$\rho_c \times 0.15$	Assumed
τ_{ic}	Rate of strain- ic quarantine-exposed individuals become I_{ic}	$\rho_{ic} \times 0.15$	Assumed
ϕ_i	Recovery rate of strain- i quarantined individuals	[0.08,0.14]	[41]
ϕ_c	Recovery rate of strain- c quarantined individuals	[0.08,0.14]	[41]
ϕ_{ic}	Recovery rate of strain- ic quarantined individuals	[0.08,0.14]	Assumed
γ_i	Recovery rate of strain- i infected individuals	[0.28,0.38]	[41]
γ_c	Recovery rate of strain- c infected individuals	[0.28,0.38]	[41]
γ_{ic}	Recovery rate of co-infected individuals	[0.28,0.38]	Assumed
η_i	Strain- i immunity rate	[0, 1]	[31]
η_c	Strain- c immunity rate	[0, 1]	[31]
δ_i	Death rate due to strain- i	[0.001,0.1]	[15]
δ_c	Death rate due to strain- c	[0.001,0.1]	[15]
δ_{ic}	Death rate due to co-infection	[0.001,0.1]	Assumed
μ	natural death rate	[0.001, 0.1]	Assumed

Table 2
Model Parameters

3.1.1. Disease-free equilibrium (DFE). The DFE of model (3.1) is given by

$$(3.3) \quad \mathbf{E}_k^0 = (S_k^0, E_k^0, I_k^0, Q_k^0, R_k^0) = \left(\frac{\Lambda}{\mu}, 0, 0, 0, 0 \right).$$

It is well-known that the local stability of the DFE is associated with the disease reproduction number. Thus, to characterize the reproduction number corresponding to (2.3), we have to look at the local stability of (3.3). Using notations in [42], we linearise the positive candidates of the infection terms, F , and a non-singular M -matrix, V , to obtain

$$F = \begin{pmatrix} 0 & \frac{S_k^0}{N_k^0} \beta_k & \frac{S_k^0}{N_k^0} \beta_k \\ 0 & 0 & 0 \\ 0 & 0 & 0 \end{pmatrix} \quad \text{and} \quad V = \begin{pmatrix} \mathbf{p}_k & 0 & 0 \\ -\rho_k & \mathbf{q}_k & -\tau_k \\ -\alpha_k & -\sigma_k & \mathbf{r}_k \end{pmatrix}, \quad \text{respectively.}$$

It follows from [9, 42] that the maximum absolute value of the next-generation matrix, FV^{-1} , is the quarantine reproduction number (QRN) defined as

$$(3.4) \quad \tilde{\mathcal{R}}_k^q = \rho(FV^{-1}) = \frac{\alpha_k \beta_k \mathbf{q}_k + \beta_k \rho_k \sigma_k + \alpha_k \beta_k \tau_k + \mathbf{r}_k \beta_k \rho_k}{\mathbf{p}_k (\dot{\mathbf{q}}_k \mathbf{r}_k + \tilde{\mathbf{r}}_k \sigma_k)}$$

where

$$\tilde{\mathbf{r}}_k = \phi_k + \delta_k + \mu, \quad \dot{\mathbf{q}}_k = \gamma_k + \delta_k + \mu, \quad \text{and } k = c \text{ or } i.$$

The QRN, $\tilde{\mathcal{R}}_k^q$, gives the secondary infections generated by an individual infected with a single pathogen in a population when the fractions of exposed and infected individuals are restricted. Applying the long-established Theorem 2 in [42], we summarize these results in the following lemma:

Lemma 3.1. *The DFE of the model (3.1) always exists. If $\tilde{\mathcal{R}}_k^q < 1$ hold, the \mathbf{E}_k^0 is locally asymptotically stable (LAS) or unstable otherwise.*

Results stated in Lemma 3.1 imply the pathogen can be removed from the population if $\tilde{\mathcal{R}}_k^q < 1$. When the threshold exceeds unity, the pathogen can invade the disease-free state. That is, the \mathbf{E}_k^0 will change its stability from stable to unstable, and the new positive endemic will appear if the initial size of the infectious is sufficiently large. Ensuring the removal of the pathogen in the community does not depend on the initial conditions showing that the DFE is globally asymptotically stable is necessary [44].

3.1.2. Global Stability of the DFE- (\mathbf{E}_k^0) . We analyze the global stability of the disease-free-equilibrium, \mathbf{E}_k^0 , using the approach as stated by [9]. In the form of Equation 3.1 in [9], we write system (3.1) as:

$$(3.5) \quad \frac{d\mathbf{x}}{dt} = F(\mathbf{x}, \mathbf{I}), \quad \frac{d\mathbf{I}}{dt} = G(\mathbf{x}, \mathbf{I}),$$

where $\mathbb{R}^2 \ni \mathbf{x} = (S, R_k)^T$ (with T denoting transpose), is a vector of uninfected individuals, and $\mathbb{R}^3 \ni \mathbf{I} = (E_k, I_k, Q_k)^T$, is a vector of infected individuals. We denote the DFE, $\mathbf{E}_k^0 = (\mathbf{x}^*, 0, 0, 0)$ where \mathbf{x}^* define the DFE of system $d\mathbf{x}/dt$. Moreover, we state the following conditions:

H1: For $F(\mathbf{x}, \mathbf{I})|_{\mathbf{x}^*}$, \mathbf{x}^* is globally asymptotically stable (GAS),

H2: $G(\mathbf{x}, \mathbf{I}) = A\mathbf{I} - \hat{G}(\mathbf{x}, \mathbf{I})$, $\hat{G}(\mathbf{x}, \mathbf{I}) \geq 0$ for $(\mathbf{x}, \mathbf{I}) \in \mathcal{C}_k$,

where $A = G(\mathbf{x}^*, 0)$ is a Metzler matrix. If the system (3.1) satisfies the two assumptions, the following assertion result holds.

Theorem 3.2. *The DFE $\mathbf{E}_k^0 = (\mathbf{x}^*, 0, 0, 0)$ of system (3.5), equivalent to (3.1) is GAS if assumptions **H1** and **H2** holds and that $\tilde{\mathcal{R}}_k^q < 1$ (LAS).*

Proof. We have shown in subsection 3.1.1 that $\tilde{\mathcal{R}}_k^q < 1$ (LAS), thus, we now prove for assumptions **H1** and **H2** only. From (3.5), we have

$$F(\mathbf{x}, 0) = \begin{pmatrix} \Lambda - \mu S \\ 0 \end{pmatrix}, \quad A = \begin{pmatrix} -\mathbf{p}_k & \beta_k & \beta_k \\ \rho_k & -\mathbf{q}_k & \tau_k \\ \alpha_k & \sigma_k & -\mathbf{r}_k \end{pmatrix},$$

and,

$$\hat{G}(\mathbf{x}, \mathbf{I}) = \begin{pmatrix} \beta_k I_k (1 - \frac{S}{N}) + \beta_k Q_k (1 - \frac{\Omega_k S}{N}) \\ 0 \\ 0 \end{pmatrix}.$$

Since $\Omega_k \in (0, 1]$ and $0 \leq \Omega_k S \leq S \leq N$ then $\hat{G}(\mathbf{x}, \mathbf{I}) \geq 0$ (**H2** holds). Moreover,

$$\lim_{t \rightarrow \infty} F(\mathbf{x}(t), \mathbf{I}(t))|_{\mathbf{x}^*} = \lim_{t \rightarrow \infty} F(\mathbf{x}(t), 0) = \left(\frac{\Lambda}{\mu}, 0 \right) = \mathbf{x}^*, \quad \mathbf{H1} \text{ holds.} \quad \blacksquare$$

We state these results in the subsequent proposition:

Proposition 3.3. *System (3.1) has the DFE, $\mathbf{E}_k^0 = (\Lambda/\mu, 0, 0, 0)$. Whenever $\tilde{\mathcal{R}}_k^q \leq 1$ the \mathbf{E}_k^0 is GAS. Otherwise, a unique positive endemic equilibrium is stable if $\tilde{\mathcal{R}}_k^q > 1$.*

3.1.3. Endemic equilibrium of the SSM. We now settle the strain-*c* (and *i*) endemic equilibria of the model (3.1). We denoted this equilibrium by

$$\tilde{\mathbf{E}}_k^* = \left[\frac{S_k^*}{N_k^*}, \frac{E_k^*}{N_k^*}, \frac{I_k^*}{N_k^*}, \frac{Q_k^*}{N_k^*}, \frac{R_k^*}{N_k^*} \right] = \left[\tilde{S}_k^*, \tilde{E}_k^*, \tilde{I}_k^*, \tilde{Q}_k^*, \tilde{R}_k^* \right].$$

We express the variables $\tilde{S}_k^*, \tilde{E}_k^*, \tilde{I}_k^*, \tilde{Q}_k^*$ and \tilde{R}_k^* in terms of $\tilde{\xi}_k^*$ as

$$(3.6) \quad \begin{aligned} \tilde{S}_k^* &= \frac{\Lambda}{\tilde{\xi}_k^* + \mu}, & \tilde{E}_k^* &= \frac{\Lambda}{\mathbf{p}_k} \frac{\tilde{\xi}_k^*}{\tilde{\xi}_k^* + \mu}, & \tilde{I}_k^* &= W_{1k} \frac{\tilde{\xi}_k^*}{\tilde{\xi}_k^* + \mu}, \\ \tilde{Q}_k^* &= W_{2k} \frac{\tilde{\xi}_k^*}{\tilde{\xi}_k^* + \mu}, & \tilde{R}_k^* &= \frac{\phi_k}{\mu} \tilde{Q}_k^* + \frac{\gamma_k}{\mu} \tilde{I}_k^*, & N_k^* &= \frac{\Lambda}{\mu} \frac{\tilde{\xi}_k^*}{\tilde{\xi}_k^* + \mu} (1 - \tilde{\Phi}_k) \end{aligned}$$

where;

$$\begin{aligned} W_{1k} &= \frac{\mathbf{r}_k \rho_k \Lambda + \alpha_k \tau_k \Lambda}{\mathbf{p}_k (\dot{\mathbf{q}}_k \mathbf{r}_k + \tilde{\mathbf{r}}_k \sigma_k)}, & W_{2k} &= \frac{\mathbf{q}_k \alpha_k \Lambda + \sigma_k \rho_k \Lambda}{\mathbf{p}_k (\dot{\mathbf{q}}_k \mathbf{r}_k + \tilde{\mathbf{r}}_k \sigma_k)}, \\ \tilde{\Phi}_k &= \left[\frac{\alpha_k \delta_k \mathbf{q}_k + \delta_k \mathbf{r}_k \rho_k + \delta_k \rho_k \sigma_k + \alpha_k \delta_k \tau_k}{\mathbf{p}_k (\dot{\mathbf{q}}_k \mathbf{r}_k + \tilde{\mathbf{r}}_k \sigma_k)} \right], & \tilde{\xi}_k^* &= \frac{\beta_k (I_k^* + (1 - \omega_k I_k^*) Q_k^*)}{N_k^*}. \end{aligned}$$

Let us now eliminate $\tilde{I}_k^*, \tilde{Q}_k^*$ and N_k^* from the expression of $\tilde{\xi}_k^*$ with their corresponding expressions in (3.6) to have the following cubic equation:

$$(3.7) \quad \tilde{\xi}_k^* (a_2 \tilde{\xi}_k^{*2} + a_1 \tilde{\xi}_k^* + a_0) = 0,$$

where;

$$\begin{aligned} a_2 &= (1 - \tilde{\Phi}_k)\Lambda, \\ a_1 &= W_{1k}W_{2k}\omega_k\beta_k\mu + (1 - \tilde{\Phi}_k)\Lambda\mu + (1 - \tilde{\mathcal{R}}_k^q)\Lambda\mu, \\ a_0 &= \mu^2(1 - \tilde{\mathcal{R}}_k^q)\Lambda. \end{aligned}$$

By inspection, it is easy to see that the one root is $\xi_{k1}^* = 0$, a disease-free equilibrium. To get the other two roots, we solve the quadratic equation inside the brackets of Equation (3.7).

Using the Routh–Hurwitz conditions on the second order polynomial [30], we analyze the quadratic (3.7) for possible steady states solutions around $\tilde{\mathcal{R}}_k^q$. *It follows that whenever $a_i < 0$, $i = 0, 1, 2$, all roots of the (3.7) are non-negative or have positive real-parts.* The parameter $\tilde{\Phi}_k$ gives the total proportion of people who will die from the disease. From a practical point of view, not all individuals in the population will die from the disease, so it is reasonable to assume that $\tilde{\Phi}_k \in (0, 1)$: implies a_2 is strictly positive. If $\tilde{\mathcal{R}}_k^q = 1$, in this case $a_0 = 0$ and $a_1 > 0$. This implies the quadratic of (3.7) has a single negative root, namely, $\xi_k^* = -a_1/a_2$. Moreover, if $\tilde{\mathcal{R}}_k^q > 1$, mathematically in this case, the quadratic has two real roots, $(-a_1 \pm \sqrt{a_1^2 + 4a_2a_0})/2a_2$: one root is positive, of course, this makes sense biologically. It gives a stable disease state. The second root is negative. Mathematically, it is defined, but, biologically is paradoxical. Finally, a_0 and a_1 are positive if $\tilde{\mathcal{R}}_k^q$ is less than unity. This imply that no positive root(s) exists whenever $\tilde{\mathcal{R}}_k^q < 1$. Consequently, no backward bifurcation. Plotting the $(\tilde{\mathcal{R}}_k^q, \xi_k^*)$ relationship (see Figure 2) provides a means of determining possible steady-states and the forward bifurcation at $\tilde{\mathcal{R}}_k^q = 1$. We summarize the results in the following theorem.

Theorem 3.4. *Model (3.1), there exists a unique and positive endemic equilibrium (given by (3.6)) if and only if $\tilde{\mathcal{R}}_k^q > 1$. Otherwise the DFE is GAS.*

3.1.4. Stability and Bifurcation of the SSM with imperfect quarantine . For a rigorous proof of local stability and non-existence of backward bifurcation of the endemic equilibrium established in Theorem 3.4, we implement the Centre Manifold Theory as described by Castillo-Chavez and Song [11]. For notations simplicity we set $S = x_1$, $E_k = x_2$, $I_k = x_3$, $Q_k = x_4$, and $R_k = x_5$, so that $N_k = \sum_{n=1}^5 x_n$. In vector form with $X = (x_1, x_2, x_3, x_4, x_5)^T$ and $\frac{dX}{dt} = G = (g_1, g_2, g_3, g_4, g_5)^T$, we can write system (3.1) as

$$(3.8) \quad G(\Lambda, \mu, \rho_k, \alpha_k, \sigma_k, \tau_k, \phi_k, \gamma_k, \mathbf{p}_k, \mathbf{q}_k, \mathbf{r}_k) = \begin{pmatrix} \Lambda - \xi_k x_1 - \mu x_1 \\ \xi_k x_1 - \mathbf{p}_k x_2 \\ \rho_k x_2 + \tau_k x_4 - \mathbf{q}_k x_3 \\ \alpha_k x_2 - \mathbf{r}_k x_4 + \sigma_k x_3 \\ \phi_k x_4 + \gamma_k x_3 - \mu x_5 \end{pmatrix}.$$

Jacobian matrix of system (3.8) about the steady-state $\mathbf{E}_k^0 = (\frac{\Lambda}{\mu}, 0, 0, 0, 0)$ is given by

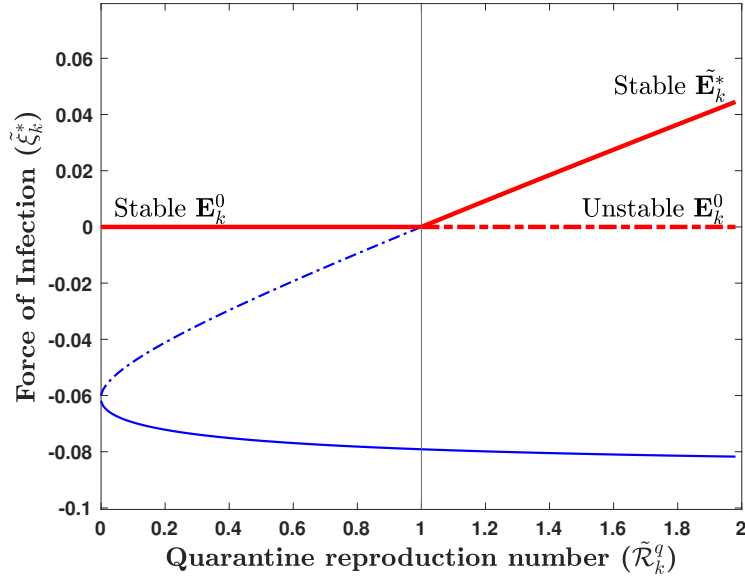


Figure 2. Schematic graphical solution $\tilde{\xi}_k^*$ of (3.7) with respect to the bifurcation parameter $\tilde{\mathcal{R}}_k^q$. Thick and dotted lines denote the stable and unstable equilibria, respectively. For $\tilde{\mathcal{R}}_k^q < 1$, there is no positive equilibrium and the disease-free \mathbf{E}_k^0 is stable. For $\tilde{\mathcal{R}}_k^q > 1$, there are two equilibria, of which one is positive and the disease-free \mathbf{E}_k^0 is unstable. Parameters used are $\beta_k \in [0.0001, 6]$, $\omega_k = 0.6$, $\Lambda = 7.2$, $\alpha_k = 1$, $\sigma_k = 2$, $\tau_k = 0.09$, $\phi_k = 5$, $\mu = 0.06$, $\delta_k = 0.09$, and $\gamma_k = 0.1$.

$$(3.9) \quad J(\mathbf{E}^0)|_{\beta_k^*} = \begin{pmatrix} -\mu & 0 & -\beta_k^* & -\beta_k^* & 0 \\ 0 & -\mathbf{p}_k & \beta_k^* & \beta_k^* & 0 \\ 0 & \rho_k & -\mathbf{q}_k & \tau_k & 0 \\ 0 & \alpha_k & -\sigma_k & -\mathbf{r}_k & 0 \\ 0 & 0 & -\gamma_k & \phi_k & -\mu \end{pmatrix}.$$

where β_k^* is the bifurcation parameter defined as,

$$\beta_k^* = \frac{\mathbf{p}_k(\dot{\mathbf{q}}_k \mathbf{r}_k + \tilde{\mathbf{r}}_k \sigma_k)}{\alpha_k \mathbf{q}_k + \rho_k \sigma_k + \alpha_k \tau_k + \mathbf{r}_k \rho_k}.$$

With β_k^* , we revealed that the Jacobian matrix (3.9) has a simple zero eigenvalue and that all other eigenvalues are negative. Further, a little algebra shows that the right eigenvectors of (3.9) associated with zero eigenvalues given by $w = [w_1, w_2, w_3, w_4, w_5]^T$ are;

$$w_1 = \frac{-b_1}{b_5}, \quad w_2 = \frac{\mu b_1}{\mathbf{p}_k b_5}, \quad w_3 = \frac{\mu b_3}{b_5}, \quad w_4 = \frac{\mu b_2}{b_5}, \quad w_5 = 1.$$

Similarly, the left eigenvector associated with a zero eigenvalue at β_k^* given by

$$v = [v_1, v_2, v_3, v_4, v_5]$$

are;

$$v_1 = 0, \quad v_2 = \frac{(b_2 + b_3)v_3}{b_4}, \quad v_3 = v_3 > 0, \quad v_4 = \frac{\mathbf{q}_k + \tau_k}{\sigma_k + \mathbf{r}_k}, \quad v_5 = 0,$$

where,

$$\begin{aligned} b_1 &= \mathbf{p}_k(\dot{\mathbf{q}}_k \mathbf{r}_k + \tilde{\mathbf{r}}_k \sigma_k), & b_2 &= \alpha_k \mathbf{q}_k + \rho_k \sigma_k, & b_3 &= \alpha_k \tau_k + \mathbf{r}_k \rho_k, \\ b_4 &= \sigma_k \mathbf{p}_k + \mathbf{r}_k \mathbf{p}_k, & b_5 &= \phi_k b_2 + \gamma_k b_3. \end{aligned}$$

3.1.5. Computation of bifurcation coefficients. Despite the non-zero values vectors v_3 and v_4 , the second derivatives of their corresponding functions are zero. Thus, g_2 is the only function required to determine the sign of a and b . The non-zero second partial derivatives of g_2 evaluated at the DFE are:

$$(3.10) \quad \begin{aligned} \frac{\partial^2 g_2}{\partial x_2 \partial x_3} &= -\frac{\mu \beta_k^*}{\Lambda}, & \frac{\partial^2 g_2}{\partial x_3^2} &= -\frac{2\mu \beta_k^*}{\Lambda}, \\ \frac{\partial^2 g_2}{\partial x_3 \partial x_4} &= -\beta_k^* \omega_k - \frac{2\mu \beta_k^*}{\Lambda}, & \frac{\partial^2 g_2}{\partial x_3 \partial x_5} &= -\frac{\mu \beta_k^*}{\Lambda}, & \frac{\partial^2 g_2}{\partial x_3 \partial \beta_k^*} &= 1. \end{aligned}$$

Hence, the coefficients

$$\begin{aligned} a &= \sum_{l,i,j=1}^5 v_l w_i w_j \frac{\partial^2 g_l}{\partial x_i \partial x_j}(0,0), \\ &= -\frac{(b_2 + b_3)}{b_4} v_3 w_3 \mu \beta_k^* \left(\frac{b_1}{\Lambda \mathbf{p}_k b_5} + \frac{2\mu b_3}{\Lambda b_5} + \frac{\mu b_2 \omega_k}{b_5} + \frac{2\mu b_2}{\Lambda b_5} + \frac{1}{\Lambda} \right) < 0, \end{aligned}$$

and

$$b = \sum_{l,i=1}^5 v_l w_i \frac{\partial^2 g_l}{\partial x_i \partial \beta_k^*}(0,0) = v_2 w_3 \frac{\partial^2 g_2}{\partial x_3 \partial \beta_k^*} = \frac{(b_2 + b_3)}{b_4} v_3 w_3 > 0.$$

Since $a < 0$ and $b > 0$, there is no backward bifurcation. As pointed out by Castillo et. al, [11] in item (iv) of Theorem 4.1, we establish the following theorem to rephrase the outcomes on the stability of endemic equilibrium and bifurcation of the model (3.1).

Theorem 3.5. Consider model (3.1), equivalently to (3.8), and assume $\Omega_k \in (0, 1]$.

- i. When the parameter β_k shifts from negative to positive, \mathbf{E}_k^0 will change its stability from stable to unstable. Alike, $\tilde{\mathbf{E}}_k^*$ changes from a negative to a positive and LAS.
- ii. Provided $a < 0$ and $b > 0$, the model in fact has forward bifurcation at $\tilde{\mathcal{R}}_k^q = 1$.

3.2. Analysis of Multiple-Strain model (MSM) with no co-infection. Here, we present the mathematical investigation of the model (2.3) when $I_{ic} = 0$ but $I_i \neq 0$ and $I_c \neq 0$. The consequential model system (3.11), has four equations less than the original, (2.3):

$$(3.11) \quad \begin{aligned} S'(t) &= \Lambda - \xi_i S - \xi_c S - \mu S, & Q'_i(t) &= \alpha_i E_i - \mathbf{r}_i Q_i + \sigma_i I_i, \\ E'_i(t) &= \xi_i S - \mathbf{p}_i E_i + \eta_c R_c \xi_i, & Q'_c(t) &= \alpha_c E_c - \mathbf{r}_c Q_c + \sigma_c I_c, \\ E'_c(t) &= \xi_c S - \mathbf{p}_c E_c + \eta_i R_i \xi_c, & R'_i(t) &= \phi_i Q_i + \gamma_i I_i - \eta_i R_i \xi_c - \mu R_i, \\ I'_i(t) &= \rho_i E_i + \tau_i Q_i - \mathbf{q}_i I_i, & R'_c(t) &= \phi_c Q_c + \gamma_c I_c - \eta_c R_c \xi_i - \mu R_c, \\ I'_c(t) &= \rho_c E_c + \tau_c Q_c - \mathbf{q}_c I_c, \end{aligned}$$

3.2.1. DFE. The disease-free equilibrium of model (3.11) is given by

$$\mathbf{\ddot{E}}^0 = (\ddot{S}^0, \ddot{E}_i^0, \ddot{E}_c^0, \ddot{I}_i^0, \ddot{I}_c^0, \ddot{Q}_i^0, \ddot{Q}_c^0, \ddot{R}_i^0, \ddot{R}_c^0) = \left(\frac{\Lambda}{\mu}, 0, 0, 0, 0, 0, 0, 0, 0 \right).$$

We calculate the reproduction number(s) and state the local stability of the disease-free equilibrium, $\mathbf{\ddot{E}}^0$. With a similar approach as in subsection 3.1.1, we found two reproduction numbers that do not depend on each other. Symbolically, we show them as

$$(3.12) \quad \tilde{\mathcal{R}}^q = \max\{\tilde{\mathcal{R}}_c^q, \tilde{\mathcal{R}}_i^q\},$$

where

$$\tilde{\mathcal{R}}_c^q = \frac{\alpha_c \beta_c \mathbf{q}_c + \beta_c \rho_c \sigma_c + \alpha_c \beta_c \tau_c + \mathbf{r}_c \beta_c \rho_c}{\mathbf{p}_c (\dot{\mathbf{q}}_c \mathbf{r}_c + \tilde{\mathbf{r}}_c \sigma_c)}, \quad \text{and,} \quad \tilde{\mathcal{R}}_i^q = \frac{\alpha_i \beta_i \mathbf{q}_i + \beta_i \rho_i \sigma_i + \alpha_i \beta_i \tau_i + \mathbf{r}_i \beta_i \rho_i}{\mathbf{p}_i (\dot{\mathbf{q}}_i \mathbf{r}_i + \tilde{\mathbf{r}}_i \sigma_i)}.$$

We then state the following proposition:

Proposition 3.6. *The DFE of the model (3.11) always exists. If $\max\{\tilde{\mathcal{R}}_c^q, \tilde{\mathcal{R}}_i^q\} < 1$ hold, $\mathbf{\ddot{E}}^0$ is locally asymptotically stable (LAS). Otherwise, it is unstable.*

Proposition 3.6 suggests that if $\tilde{\mathcal{R}}_c^q < 1$ and $\tilde{\mathcal{R}}_i^q > 1$ then strain- i will dominate and drives strain- c to extinction. On contrarily, if $\tilde{\mathcal{R}}_i^q < 1$ and $\tilde{\mathcal{R}}_c^q > 1$ then strain- c will dominate and drives strain- i to extinction. Moreover, if the reproduction number of each strain exceeds the unity ($\tilde{\mathcal{R}}_i^q > 1$ and $\tilde{\mathcal{R}}_c^q > 1$), then competition; strain- c and strain- i will compete for susceptible individuals. In this case, the strain with a large reproduction number outcompete the other. The competition will exhibit the so-called exclusive principle if the competed strain extinct [28]. For the principle to satisfy the result stated in Proposition 3.6 must hold globally. We provide the proof given in Appendix B and use Theorem 8.2 stated in [28], to summarize the results:

Proposition 3.7. *The DFE, $\mathbf{\ddot{E}}_k^0$ of system (3.11) is globally asymptotically stable (GAS) if $\max\{\tilde{\mathcal{R}}_c^q, \tilde{\mathcal{R}}_i^q\} \leq 1$. Contrarily, when $\tilde{\mathcal{R}}_c^q > 1$ and or $\tilde{\mathcal{R}}_i^q > 1$ strain with the largest reproduction number dominates the other and drives them to extinction.*

3.2.2. Dominance endemic equilibrium. Let $\mathbf{\ddot{E}}_c^d$ and $\mathbf{\ddot{E}}_i^d$ be strain- c and strain- i dominance equilibria of the model (3.11) when $\Omega_k \in (0, 1]$. Starting by deducing that $E_i = I_i = Q_i = R_i = 0$. The obtained equations that satisfy $\mathbf{\ddot{E}}_c^d$ are indeed similar to the model system (3.1) at equilibrium on replacing c by k . Thus analyzing the resulting model in a similar way to that used in subsection 3.1.3, we have

$$(3.13) \quad \tilde{\mathbf{E}}_c^d = \left[\tilde{S}_c^d, 0, \tilde{E}_c^d, 0, 0, \tilde{I}_c^d, 0, 0, \tilde{Q}_c^d, 0, 0, \tilde{R}_c^d, 0 \right].$$

Similarly, in the case when $E_c = I_c = Q_c = R_c = 0$ we obtain the strain- i dominance equilibrium; namely,

$$(3.14) \quad \tilde{\mathbf{E}}_i^d = \left[\tilde{S}_i^d, \tilde{E}_i^d, 0, 0, \tilde{I}_i^d, 0, 0, \tilde{Q}_i^d, 0, 0, \tilde{R}_i^d, 0, 0 \right].$$

Note, the non-zero variables: $\tilde{S}_c^d, \tilde{E}_c^d, \tilde{I}_c^d, \tilde{Q}_c^d$ and \tilde{R}_c^d in Equation (3.13) and $\tilde{S}_i^d, \tilde{E}_i^d, \tilde{I}_i^d, \tilde{Q}_i^d$ and \tilde{R}_i^d in Equation (3.14) are solutions obtained by replacing them with the corresponding expressions of $\tilde{S}_k^*, \tilde{E}_k^*, \tilde{I}_k^*, \tilde{Q}_k^*$, and \tilde{R}_k^* presented in (3.6) when $k = c$ or $k = i$.

3.2.3. Invasion reproduction numbers-(IRN). To investigate the local stability of $\tilde{\mathbf{E}}_k^d$, the endemic equilibrium in the absence of one pathogen, we compute the invasion reproduction numbers for strain- i (and strain- c), ${}_i\tilde{\mathcal{R}}_c^q$ (and ${}_c\tilde{\mathcal{R}}_i^q$), respectively. The quantity ${}_i\tilde{\mathcal{R}}_c^q$ (or ${}_c\tilde{\mathcal{R}}_i^q$) is used to measure the ability of strain- i (or strain- c) to invade a system at the equilibrium of the strain- c (or strain- i). See, for example, [28, 42] described various approaches to calculate the IRN. The method we use to obtain ${}_i\tilde{\mathcal{R}}_c^q$ is the next-generation approach (included in the Appendix C). The expression of ${}_i\tilde{\mathcal{R}}_c^q$, simplifies to

$$(3.15) \quad {}_i\tilde{\mathcal{R}}_c^q = \left[\tilde{S}_c^* + \tilde{R}_c^* \eta_c \right] \tilde{\mathcal{R}}_i^q.$$

Analogously, we define the strain- c invasion reproduction number, ${}_c\tilde{\mathcal{R}}_i^q$, under the assumption that the strain- i is resident to obtain

$$(3.16) \quad {}_c\tilde{\mathcal{R}}_i^q = \left[\tilde{S}_i^* + \tilde{R}_i^* \eta_i \right] \tilde{\mathcal{R}}_c^q.$$

From Equation (3.15), we notice that the term $\tilde{S}_c^* \tilde{\mathcal{R}}_i^q$ provides secondary cases of susceptible individuals that one individual infected with strain- i can produce in the population. The term $\tilde{R}_c^* \eta_c \tilde{\mathcal{R}}_i^q$ provide the secondary cases one strain- i infected individual can produce in proportions of the individual recovered from strain- c . The interpretation of Equation (3.16) is treated similarly to (3.15). We then compile the results on the existence and stability of $\tilde{\mathbf{E}}_c^d$ (and $\tilde{\mathbf{E}}_i^d$) of the model (3.11) in the following proposition:

Proposition 3.8. *Assume that $j \neq k = c$ or i . If $\tilde{\mathcal{R}}_k^q > 1$, then the endemic equilibrium $\tilde{\mathbf{E}}_k^d$ exists. Whenever ${}_j\tilde{\mathcal{R}}_k^q > 1$, the equilibrium $\tilde{\mathbf{E}}_k^d$ is unstable. Otherwise, the equilibrium $\tilde{\mathbf{E}}_k^d$ is LAS if the invasion reproduction number ${}_j\tilde{\mathcal{R}}_k^q < 1$.*

3.2.4. Coexistence of endemic with no co-infection. To obtain the analytical solution, we assume complete protection of recovered individuals against the secondary pathogen, that is, $\eta_c = \eta_i = 0$. Let $\tilde{\mathbf{E}}^*$ be the coexistence equilibrium. In terms of the force of infections, $\ddot{\xi}_i^*$ and $\ddot{\xi}_c^*$, defined as

$$(3.17) \quad \ddot{\xi}_i^* = \frac{\beta_i(\ddot{I}_i + (1 - \omega_i \ddot{I}_i) \ddot{Q}_i)}{\ddot{N}_t}, \quad \text{and} \quad \ddot{\xi}_c^* = \frac{\beta_c(\ddot{I}_c + (1 - \omega_c \ddot{I}_c) \ddot{Q}_c)}{\ddot{N}_t}$$

where $\ddot{N}_t = (\Lambda - (\delta_i(\ddot{I}_i + \ddot{Q}_i)) - \delta_c(\ddot{I}_c + \ddot{Q}_c))/\mu$, the non-zero variables of the equilibrium

$$\begin{aligned}\ddot{\mathbf{E}}^* &= \left[\frac{\ddot{S}}{\ddot{N}_t}, \frac{\ddot{E}_i}{\ddot{N}_t}, \frac{\ddot{E}_c}{\ddot{N}_t}, 0, \frac{\ddot{I}_i}{\ddot{N}_t}, \frac{\ddot{I}_c}{\ddot{N}_t}, 0, \frac{\ddot{Q}_i}{\ddot{N}_t}, \frac{\ddot{Q}_c}{\ddot{N}_t}, 0, \frac{\ddot{R}_i}{\ddot{N}_t}, \frac{\ddot{R}_c}{\ddot{N}_t}, 0 \right] \\ &= \left[\ddot{S}^*, \ddot{E}_i^*, \ddot{E}_c^*, 0, \ddot{I}_i^*, \ddot{I}_c^*, 0, \ddot{Q}_i^*, \ddot{Q}_c^*, 0, \ddot{R}_i^*, \ddot{R}_c^*, 0 \right],\end{aligned}$$

satisfying the successive equations:

$$(3.18) \quad \begin{aligned}\ddot{S}^* &= \frac{\Lambda}{\ddot{\xi}_i^* + \ddot{\xi}_c^* + \mu}, & \ddot{I}_i^* &= \frac{\ddot{\xi}_i^* W_{11}}{(\ddot{\xi}_i^* + \ddot{\xi}_c^* + \mu)}, & \ddot{Q}_c^* &= \frac{\ddot{\xi}_c^* W_{44}}{(\ddot{\xi}_i^* + \ddot{\xi}_c^* + \mu)}, \\ \ddot{E}_i^* &= \frac{\ddot{\xi}_i^* \Lambda}{\mathbf{p}_i(\ddot{\xi}_i^* + \ddot{\xi}_c^* + \mu)}, & \ddot{I}_c^* &= \frac{\ddot{\xi}_c^* W_{33}}{(\ddot{\xi}_i^* + \ddot{\xi}_c^* + \mu)}, & \ddot{R}_i^* &= \frac{\phi_i \ddot{Q}_i^*}{\mu} + \frac{\gamma_i \ddot{Q}_i^*}{\mu}, \\ \ddot{E}_c^* &= \frac{\ddot{\xi}_c^* \Lambda}{\mathbf{p}_c(\ddot{\xi}_i^* + \ddot{\xi}_c^* + \mu)}, & \ddot{Q}_i^* &= \frac{\ddot{\xi}_i^* W_{22}}{(\ddot{\xi}_i^* + \ddot{\xi}_c^* + \mu)}, & \ddot{R}_c^* &= \frac{\phi_c \ddot{Q}_c^*}{\mu} + \frac{\gamma_c \ddot{Q}_c^*}{\mu}.\end{aligned}$$

The parameter $W_{11} = W_{1k}$ when $(k = i)$, $W_{22} = W_{2k}$ when $(k = i)$, $W_{33} = W_{1k}$ when $(k = c)$, and $W_{44} = W_{2k}$ when $(k = c)$. Employing (3.18) we obtain, from (3.17),

$$(3.19) \quad \begin{aligned}0 &= \ddot{\xi}_i^* \left[W_{55} \omega_i \beta_i \mu \ddot{\xi}_i^* + (1 - \Phi_c) \ddot{\xi}_c^{*2} + (1 - \Phi_i) \ddot{\xi}_i^{*2} + \left[(1 - \Phi_c) + (1 - \Phi_i) \right] \ddot{\xi}_i^* \ddot{\xi}_c^* \right. \\ &\quad \left. + (1 - \Phi_c) \mu \ddot{\xi}_c^* + (1 - \Phi_i) \mu \ddot{\xi}_i^* + (1 - \tilde{\mathcal{R}}_i^q) \mu \ddot{\xi}_c^* + (1 - \tilde{\mathcal{R}}_i^q) \mu \ddot{\xi}_i^* + (1 - \tilde{\mathcal{R}}_i^q) \mu^2 \right] \\ &= f_1(\ddot{\xi}_c^*, \ddot{\xi}_i^*), \\ 0 &= \ddot{\xi}_c^* \left[W_{66} \omega_c \beta_c \mu \ddot{\xi}_c^* + (1 - \Phi_i) \ddot{\xi}_i^{*2} + (1 - \Phi_c) \ddot{\xi}_c^{*2} + \left[(1 - \Phi_i) + (1 - \Phi_c) \right] \ddot{\xi}_i^* \ddot{\xi}_c^* \right. \\ &\quad \left. + (1 - \Phi_c) \mu \ddot{\xi}_c^* + (1 - \Phi_i) \mu \ddot{\xi}_i^* + (1 - \tilde{\mathcal{R}}_c^q) \mu \ddot{\xi}_c^* + (1 - \tilde{\mathcal{R}}_c^q) \mu \ddot{\xi}_i^* + (1 - \tilde{\mathcal{R}}_c^q) \mu^2 \right] \\ &= f_2(\ddot{\xi}_c^*, \ddot{\xi}_i^*).\end{aligned}$$

where,

$$W_{55} = \left[\frac{(\mathbf{r}_i \rho_i \Lambda + \alpha_i \tau_i \Lambda)(\mathbf{q}_i \alpha_i + \sigma_i \rho_i)}{\mathbf{p}_k(\dot{\mathbf{q}}_k \mathbf{r}_k + \tilde{\mathbf{r}}_k \sigma_k)^2} \right] \quad \text{and} \quad W_{66} = \left[\frac{(\mathbf{r}_c \rho_c \Lambda + \alpha_c \tau_c \Lambda)(\mathbf{q}_c \alpha_c + \sigma_c \rho_c)}{\mathbf{p}_c(\dot{\mathbf{q}}_c \mathbf{r}_c + \tilde{\mathbf{r}}_c \sigma_c)^2} \right].$$

The fixed points, $(\ddot{\xi}_c^*, \ddot{\xi}_i^*)$ are the solutions s_1, s_2, s_3, s_4, s_5 of $f_1(\ddot{\xi}_c^*, \ddot{\xi}_i^*) = f_2(\ddot{\xi}_c^*, \ddot{\xi}_i^*) = 0$. The solution s_1 obtained when $\ddot{\xi}_c^* = \ddot{\xi}_i^* = 0$. When either $\ddot{\xi}_c^* = 0$ or $\ddot{\xi}_i^* = 0$, the obtained solutions are s_1, s_2 , and s_3 , given by

$$(3.20) \quad s_1 = (0, 0); \quad s_2 = \left(0, \frac{-b_1 \pm \sqrt{b_1^2 - 4a_1 c_1}}{2a_1} \right); \quad s_3 = \left(\frac{-b_2 \pm \sqrt{b_2^2 - 4a_2 c_2}}{2a_2}, 0 \right)$$

where,

$$\begin{aligned}a_1 &= (1 - \Phi_i); & a_2 &= (1 - \Phi_c); \\ b_1 &= W_{55} \omega_i \beta_i \mu + (1 - \tilde{\mathcal{R}}_i^q) + (1 - \Phi_i); & b_2 &= W_{66} \omega_c \beta_c \mu + (1 - \tilde{\mathcal{R}}_c^q) + (1 - \Phi_c); \\ c_1 &= (1 - \tilde{\mathcal{R}}_i^q) \mu^2; & c_2 &= (1 - \tilde{\mathcal{R}}_c^q) \mu^2.\end{aligned}$$

The first fixed point $s_1 = (0, 0)$ in (3.20) corresponds to the state when everyone in the population is susceptible. The solutions s_2 and s_3 correspond to strain- i and strain- c dominance equilibrium, respectively. For a detailed analysis of the existence and stability of such steady states, see subsection 3.2.2. Other nonzero solutions, s_4 and s_5 when $\ddot{\xi}_c^* > 0$ and $\ddot{\xi}_i^* > 0$ are described in this subsection.

Before discussing and establish condition(s) necessary for the coexistence solution(s) in Figure 3, we start by graphing solution for system (3.19) in $(\ddot{\xi}_c^*, \ddot{\xi}_i^*)$ relationship to check if the system (3.19) has at least one solution in the case $\ddot{\xi}_c^*$ and $\ddot{\xi}_i^*$ are both greater than zero. If there is no such solution, then there is no coexistence equilibrium. From the figure, it is easy to see that several solutions are possible depending on the parameter values.

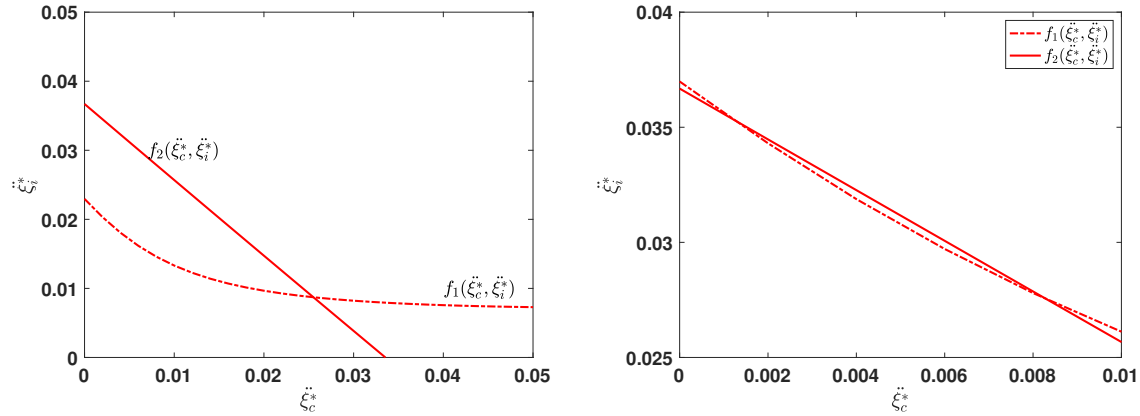


Figure 3. Possible coexistence solutions. The parameters value used for these figure are $\Lambda = 0.0004$, $\beta_c = 0.8$, $\rho_i = 0.3$, $\rho_c = 0.4$, $\alpha_i = 0.8$, $\alpha_c = 0.3$, $\sigma_i = .9$, $\sigma_c = .6$, $\tau_i = .1$, $\tau_c = .12$, $\delta_i = .1$, $\delta_c = .01$, $\mu = 0.01$, $\delta_{ic} = .1$, $\phi_i = 0.2$, $\phi_c = 0.16$, $\gamma_i = 0.2$, $\gamma_c = 0.4$, $\omega_i = 0.002$, $\omega_c = 0.05$ except for the left figure $\beta_i = 0.8$, and for the right figure $\beta_i = 1.1$.

Theorem 3.9. Suppose that each(or any) strain can invade the other population, that is ${}_i\tilde{\mathcal{R}}_c^q > 1$, and (or) ${}_c\tilde{\mathcal{R}}_i^q > 1$. System (3.11) has at least one coexistence endemic equilibrium provided that the $\min\{\tilde{\mathcal{R}}_c^q, \tilde{\mathcal{R}}_i^q\} > 1$.

Proof. Dividing each equation in (3.19) by the common factor and then adding the acquired equations, we have;

$$W_{55}\omega_i\beta_i\mu\ddot{\xi}_i^* - W_{66}\omega_c\beta_c\mu\ddot{\xi}_c^* + (\tilde{\mathcal{R}}_c^q - \tilde{\mathcal{R}}_i^q)\mu\ddot{\xi}_c^* + (\tilde{\mathcal{R}}_c^q - \tilde{\mathcal{R}}_i^q)\mu\ddot{\xi}_i^* + (\tilde{\mathcal{R}}_c^q - \tilde{\mathcal{R}}_i^q)\mu^2 = 0.$$

We assume that $\tilde{\mathcal{R}}_i^q = \tilde{\mathcal{R}}_c^q > 1$, to obtain

$$(3.21) \quad s_4 = \left(\frac{W_{55}\omega_i\beta_i\ddot{\xi}_i^*}{W_{66}\omega_c\beta_c}, \ddot{\xi}_i^* \right) \quad \text{and} \quad s_5 = \left(\ddot{\xi}_c^*, \frac{W_{66}\omega_c\beta_c\ddot{\xi}_c^*}{W_{55}\omega_i\beta_i} \right).$$

It should be noted that, s_4 and s_5 exist if and only if $\ddot{\xi}_c^* > 0$ and $\ddot{\xi}_i^* > 0$. Making usage of (3.21) and (3.19) while collecting like terms, we obtain after manipulations the following two quadratic equations:

$$(3.22) \quad \begin{aligned} a_{11}\ddot{\xi}_i^* + b_{11}\dot{\xi}_i^* + c_{11} &= 0, \\ a_{22}\ddot{\xi}_c^* + b_{22}\dot{\xi}_c^* + c_{22} &= 0, \end{aligned}$$

where

$$\begin{aligned} a_{11} &= W_{66}^2\beta_c^2\omega_c^2(1 - \Phi_i) + W_{55}W_{66}\beta_c\beta_i\omega_c\omega_i \left[(1 - \Phi_c) + (1 - \Phi_i) \right] + W_{55}^2\beta_i^2\omega_i^2(1 - \Phi_c), \\ b_{11} &= W_{55}W_{66}^2\beta_c^2\beta_i\omega_c^2\omega_i\mu + (1 - \Phi_c)W_{55}W_{66}\beta_c\beta_i\omega_c\omega_i\mu + (1 - \Phi_i)W_{66}^2\beta_c^2\omega_c^2\mu + \\ &\quad (1 - \tilde{\mathcal{R}}_i^q) \left[W_{55}W_{66}\beta_c\beta_i\omega_c\omega_i\mu + W_{66}^2\beta_c^2\omega_c^2\mu \right], \\ c_{11} &= W_{66}^2\beta_c^2\omega_c^2\mu^2(1 - \tilde{\mathcal{R}}_i^q), \end{aligned}$$

besides,

$$\begin{aligned} a_{22} &= W_{66}^2\beta_c^2\omega_c^2(1 - \Phi_i) + W_{55}W_{66}\beta_c\beta_i\omega_c\omega_i \left[(1 - \Phi_c) + (1 - \Phi_i) \right] + W_{55}^2\beta_i^2\omega_i^2(1 - \Phi_c), \\ b_{22} &= W_{55}^2W_{66}\beta_c\beta_i^2\omega_c\omega_i^2\mu + (1 - \Phi_i)W_{55}W_{66}\beta_c\beta_i\omega_c\omega_i\mu + (1 - \Phi_c)W_{55}^2\beta_i^2\omega_i^2\mu + \\ &\quad (1 - \tilde{\mathcal{R}}_c^q) \left[W_{55}W_{66}\beta_c\beta_i\omega_c\omega_i\mu + W_{55}^2\beta_i^2\omega_i^2\mu \right], \\ c_{22} &= W_{55}^2\beta_i^2\omega_i^2\mu^2(1 - \tilde{\mathcal{R}}_c^q). \end{aligned}$$

We analyze the two equations in (3.22) for possible steady states solutions around the reproduction numbers, $\tilde{\mathcal{R}}_c^q$ and $\tilde{\mathcal{R}}_i^q$. The parameters $\tilde{\Phi}_c, \tilde{\Phi}_i \in (0, 1)$. Thus a_{11} and a_{22} are strictly positive. Applying the Routh–Hurwitz criterion, it follows that when the coefficients signs of the constant terms (i.e., c_{11} and c_{22}) are negative, it follows that a positive root with a real part will exist. This is only possible whenever $\tilde{\mathcal{R}}_c^q > 1$ and $\tilde{\mathcal{R}}_i^q > 1$. ■

Note that Figure 4 is the analysis and projection of the co-exist system in (3.11) with cross-immunity onto the $(\tilde{\mathcal{R}}_c^q, \tilde{\mathcal{R}}_i^q)$ plane performed to confirm theoretical results in Theorem 3.9. Because we assumed symmetry of the model about the two strains, we also observe that the solution is symmetrical about the line $\tilde{\mathcal{R}}_c^q = \tilde{\mathcal{R}}_i^q > 1$. The boundary curves (in region $\mathbf{C}=\mathbf{C1}+\mathbf{C2}$), dotted and solid lines, are given parametrically respectively by (3.15) and (3.16). Moreover, the interactions between strain- c and $-i$ were linked by cross-immunity parameters, η_c , and η_i from each. By varying values of the cross-immunity, we observed that the larger η_i and η_c are, the larger the co-infected region. For instance, the top left figure is simply the visualization of the coexistence region obtained by setting the cross-protection rates to zero, such that $\eta_c = \eta_i = 0$. The process proceeds in two ways to obtain the remaining figures: holding one parameter to zero and increasing the other parameter or by increasing both parameters (η_c and η_i).

Besides, from the portraiture Figure 4, we obtained various regions, all of which have biological consequences. We call A a lose-lose region. In this region, all the reproduction numbers were less than one, meaning that, as time passes, all strains will die. In B, strain- i

will win, and strain-c will lose. In D, strain-c will win, but strain-i will lose. We, therefore, call the competition outcome/behavior in B and D a Win-lose competition. Next, we looked C, (a Win-win region). Here the reproduction number of each strain is large than one. Intuitively this means that each pathogen expects to come out ahead. We call the situation a Win-win competition. Further, we define a draw outcome/competition. A competition if neither strain-c nor strain-i will lose or win the competition, regardless that their reproduction numbers exceed one, see the top left figure of Figure 4. The outcome is shown by a full-dotted line (when $\tilde{\mathcal{R}}_c^q = \tilde{\mathcal{R}}_i^q > 1$).

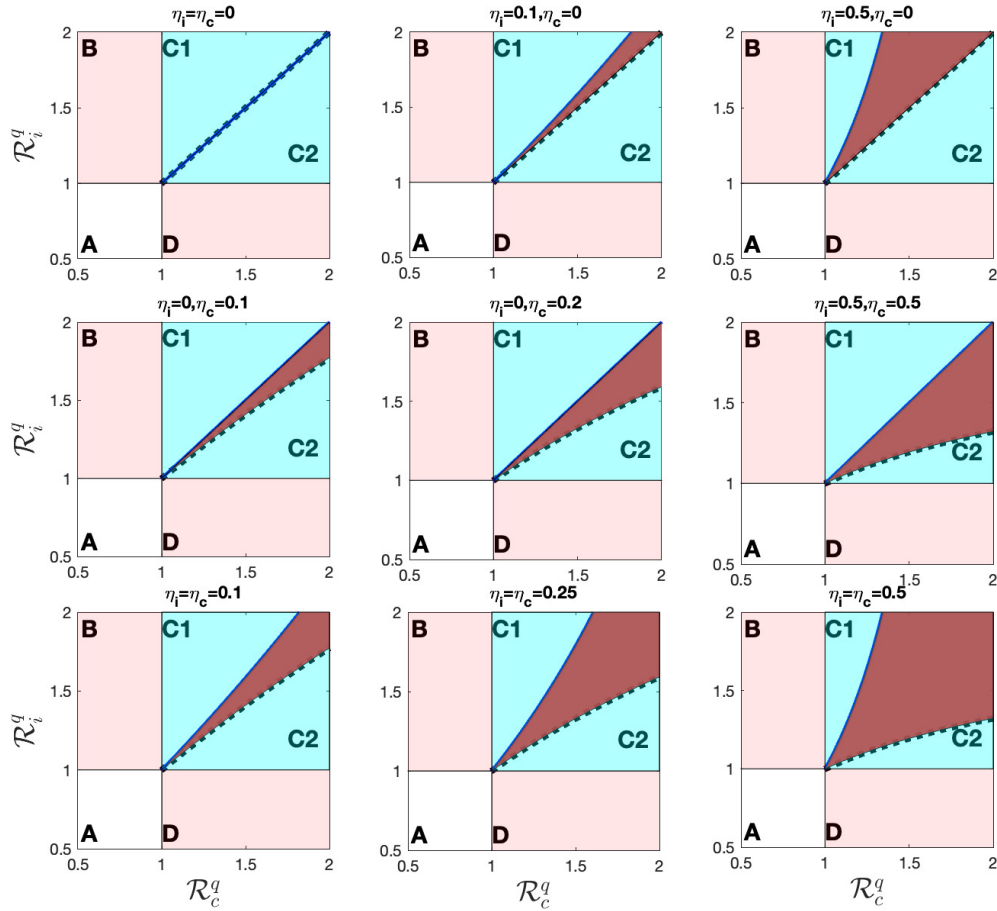


Figure 4. Dominance, competition, and co-existence regions characterized quarantine reproduction number by different values of cross-immunity, η_i and η_c . Other parameters are taken as follows: $\Lambda = 0.0004$, $\beta_c \in [0.25, 1]$, $\beta_i = 0.69$, $\rho_i = 0.5$, $\rho_c = 0.6$, $\rho_{ic} = 0.5$, $\alpha_i = 0.2$, $\alpha_c = 0.5$, $\alpha_{ic} = 0.5$, $\sigma_i = .005$, $\sigma_c = .006$, $\sigma_{ic} = .009$, $\tau_i = .05$, $\tau_c = .06$, $\tau_{ic} = .05$, $\delta_i = .001$, $\delta_c = .01$, $\mu = 0.004$, $\delta_{ic} = .1$, $\phi_i = 0.5$, $\phi_c = 0.6$, $\gamma_i = 0.2$, $\gamma_c = 0.125$, $\gamma_{ic} = 0.1$

3.3. Existence of co-infection equilibrium. Note that the analytical analysis of the two-strain model in subsection 3.2 is marked on the assumption that $E_{ic} = I_{ic} = Q_{ic} = R_{ic} = 0$. We now consider the analysis of the model system, presented in (2.3). Subsection 2.3 describe the non-negativity and boundedness of the model solution. Let us nail the stationary states. The DFE of the model is given by

$$(3.23) \quad \begin{aligned} \mathbf{E}^0 &= (S^0, E_i^0, E_c^0, E_{ic}^0, I_i^0, I_c^0, I_{ic}^0, Q_i^0, Q_c^0, Q_{ic}^0, R_i^0, R_c^0, R_{ic}^0) \\ &= \left(\frac{\Lambda}{\mu}, 0, 0, 0, 0, 0, 0, 0, 0, 0, 0, 0, 0 \right) \end{aligned}$$

Quarantine reproduction numbers are given in Equation (3.12). The local stability analysis of \mathbf{E}^0 is similar to that provided in subsection 3.2.1 except that the co-infected model (2.3) makes biological sense in \mathcal{C} , see subsection 2.3 for more details. Let

$$\begin{aligned} \tilde{\mathbf{E}}_{ic}^{**} &= \left[\frac{\hat{S}}{\hat{N}_T}, \frac{\hat{E}_i}{\hat{N}_T}, \frac{\hat{E}_c}{\hat{N}_T}, \frac{\hat{E}_{ic}}{\hat{N}_T}, \frac{\hat{I}_i}{\hat{N}_T}, \frac{\hat{I}_c}{\hat{N}_T}, \frac{\hat{I}_{ic}}{\hat{N}_T}, \frac{\hat{Q}_i}{\hat{N}_T}, \frac{\hat{Q}_c}{\hat{N}_T}, \frac{\hat{Q}_{ic}}{\hat{N}_T}, \frac{\hat{R}_i}{\hat{N}_T}, \frac{\hat{R}_c}{\hat{N}_T}, \frac{\hat{R}_{ic}}{\hat{N}_T} \right] \\ &= [S^{**}, E_i^{**}, E_c^{**}, E_{ic}^{**}, I_i^{**}, I_c^{**}, I_{ic}^{**}, Q_i^{**}, Q_c^{**}, Q_{ic}^{**}, R_i^{**}, R_c^{**}, R_{ic}^{**}], \end{aligned}$$

be the co-exist endemic equilibrium with individuals infected by strain- c and $-i$. We have seen in Theorem 3.9 that if the co-infected individuals are not present, the coexistence equilibrium, $\tilde{\mathbf{E}}^*$ occurs when $\min\{\tilde{\mathcal{R}}_c^q, \tilde{\mathcal{R}}_i^q\} > 1$ and ${}_i\tilde{\mathcal{R}}_c^q > 1$, and (or) ${}_c\tilde{\mathcal{R}}_i^q > 1$. A key question is: does this condition enough for the coexistence-endemic equilibrium "with" co-infected individuals to occur? To answer this question, we evaluate the invasion reproduction numbers when $I_{ic} \neq 0$.

3.4. Invasion reproduction number. We use the next-generation approach to derive the strain- i invasion reproduction number, ${}_i\tilde{\mathcal{I}}_c^q$ when strain- c is resident. The infectious classes are $E_i, E_{ic}, I_i, I_{ic}, Q_i$ & Q_{ic} . Procedures in Appendix C are repeated to get

$$(3.24) \quad {}_i\tilde{\mathcal{I}}_c^q = S^{**}\tilde{\mathcal{R}}_i^q + I_c^{**}\tilde{\mathfrak{X}}_i^c + R_c^{**}\eta_c\tilde{\mathcal{R}}_i^q.$$

Analogously, the strain- c invasion reproduction number, ${}_c\tilde{\mathcal{I}}_i^q$ under the assumption that strain- i is resident, respectively, is defined as

$$(3.25) \quad {}_c\tilde{\mathcal{I}}_i^q = S^{**}\tilde{\mathcal{R}}_c^q + I_i^{**}\tilde{\mathfrak{X}}_c^i + R_i^{**}\eta_i\tilde{\mathcal{R}}_c^q.$$

In (3.24) and (3.25), the first and the last terms have a similar interpretation as in subsection 3.2.3. The second terms $\tilde{\mathfrak{X}}_i^c$ and $\tilde{\mathfrak{X}}_c^i$ gives the co-infected quarantine reproduction number (CQRN) generated by strain- i and strain- c in the sub-population of strain- c infected (I_c^{**}) and strain- i infected individuals (I_i^{**}), respectively. The quantities $\tilde{\mathfrak{X}}_i^c$ and $\tilde{\mathfrak{X}}_c^i$ are given by

$$\tilde{\mathfrak{X}}_i^c = \frac{\alpha_{ic}\beta_i\mathbf{Q}_{ic} + \beta_i\rho_{ic}\sigma_{ic} + \alpha_{ic}\beta_i\tau_{ic} + \mathbf{r}_{ic}\beta_i\rho_{ic}}{\mathbf{p}_{ic}(\mathbf{Q}_{ic}\mathbf{r}_{ic} + \tilde{\mathbf{r}}_{ic}\sigma_{ic})},$$

and

$$\tilde{\mathfrak{R}}_c^i = \frac{\alpha_{ic}\beta_c\mathbf{q}_{ic} + \beta_c\rho_{ic}\sigma_{ic} + \alpha_{ic}\beta_c\tau_{ic} + \mathbf{r}_{ic}\beta_c\rho_{ic}}{\mathbf{p}_{ic}(\dot{\mathbf{q}}_{ic}\mathbf{r}_{ic} + \tilde{\mathbf{r}}_{ic}\sigma_{ic})}.$$

If $\tilde{\mathfrak{R}}_c^i < 1$ and $\tilde{\mathfrak{R}}_c^c < 1$ then in the long-run $I_i^{**}\tilde{\mathfrak{R}}_c^i \rightarrow 0$ and $I_c^{**}\tilde{\mathfrak{R}}_c^c \rightarrow 0$; this implies that co-infected sub-population will de-escalate. With these results, we establish the following theorem.

Theorem 3.10. *Assume that $\tilde{\mathcal{R}}_i^q > 1$ and $\tilde{\mathcal{R}}_c^q > 1$. The system (2.3) has a co-existence endemic equilibrium provided that ${}_i\tilde{\mathcal{I}}_c^q > 1$ and / or ${}_c\tilde{\mathcal{I}}_i^q > 1$. Moreover, the equilibrium will have co-infected individuals provided that $\tilde{\mathfrak{R}}_c^i > 1$ and or $\tilde{\mathfrak{R}}_c^c > 1$.*

Speaking broadly, model (2.3) is tedious to obtain analytical solutions. Therefore, in Figure 5, we have shown numerically calculated solutions of model (2.3) for given parameter values. We found that the strain with the large reproduction number dominates the system. Moreover, whenever the invasion reproduction number(s) is (are) bigger than one, the co-infection strain remains in the population.

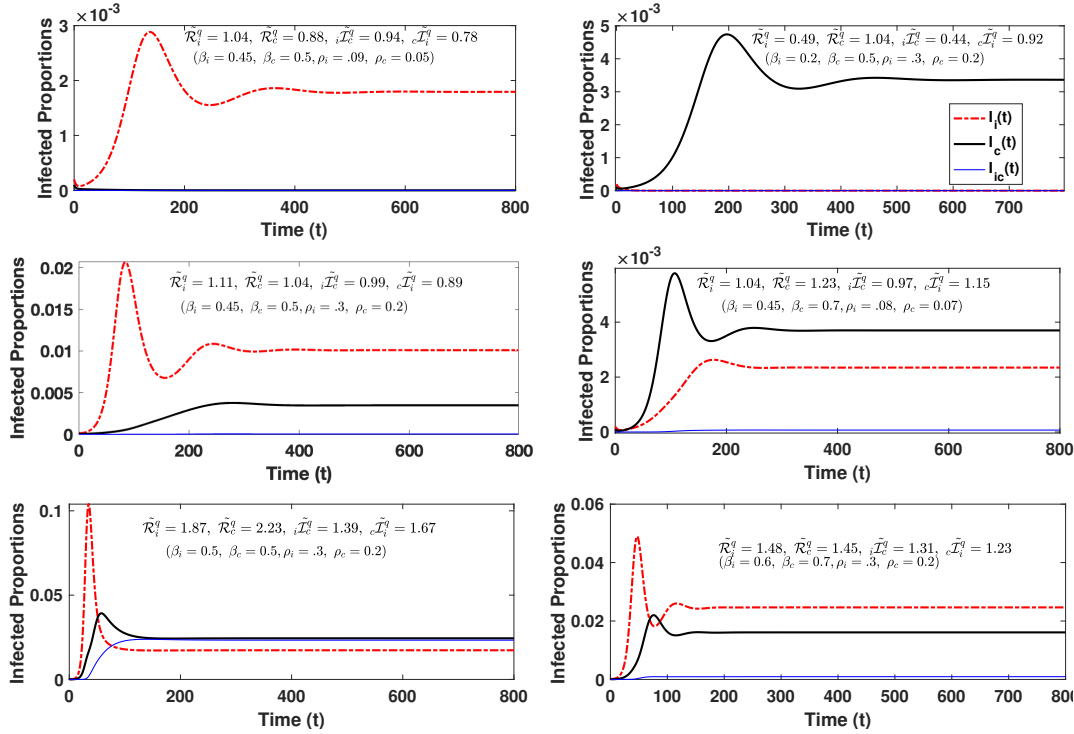


Figure 5. Co-existence of multi-strain with co-infection.

3.5. Sensitivity and the quarantine impact analysis .

3.5.1. Elasticity of Reproduction numbers. Primarily, sensitivity analysis of model parameters focuses on determining the most influential model parameters to plan the control

strategies and to give guidance to the subsequent scientific work [18, 37]. In this subsection, we aim to investigate the relative importance of each model parameter included in the reproduction numbers using the differential sensitivity analysis as described in [18]. The sensitivity coefficient, Γ_q , of the independent variable, q , and dependent variable, Q , obtained from the partial derivative of Q to q . This result gives the percentage change in the quantity Q to the percentage change in the parameter q [28] is described by the formula:

$$(3.26) \quad \Gamma_q = \frac{\partial Q}{\partial q} \times \frac{Q}{q} \approx \frac{\% \Delta Q}{\% \Delta q}$$

To assess how the model parameters impact the initial disease transmission, we performed a local sensitivity analysis in all parameters (independent variables) included in the reproduction numbers (dependent variables). The process was performed repeatedly by varying a single parameter at a time while holding the others constant. Computational outcomes are presented in Table 3.

3.5.2. Quarantine impact. We analyze the efficacy of quarantine at the initial disease transmission to determine whether or not the increase of people in the quarantine facilities can be more beneficial or useless during the epidemic. It is evident from Table 3 that the elasticity of the quantity $\tilde{\mathcal{R}}_k^q$ to its parameters is a monotonic decreasing function of α_k and σ_k . With that in mind, *we assess how the $\tilde{\mathcal{R}}_k^q$ will behave for the small and large values of these parameters.* For $\sigma_k = 0$ we evaluate the critical level of the quarantine reproduction number corresponding to the limit $\alpha_k \rightarrow 0$ and $\alpha_k \rightarrow \infty$, respectively, we have

$$(3.27) \quad \tilde{\mathcal{R}}_k^q(\alpha_k^0) = \lim_{\alpha_k \rightarrow 0} \tilde{\mathcal{R}}_k^q = \frac{\mathbf{r}_k \beta_k \rho_k}{\mathbf{p}_k \mathbf{q}_k \mathbf{r}_k}, \quad \text{and} \quad \tilde{\mathcal{R}}_k^q(\alpha_k^\infty) = \lim_{\alpha_k \rightarrow \infty} \tilde{\mathcal{R}}_k^q = \frac{\beta_k \mathbf{q}_k + \beta_k \tau_k}{\mathbf{q}_k \mathbf{r}_k},$$

where $k = c$ or i . The first and the second Equations of (3.27), correspondingly, give the maximum and the minimum number of secondary cases generated when only exposed are quarantined. On the other hand, for a fixed $\alpha_k = 0$ the critical levels of the QRN corresponds to the limit $\sigma_k \rightarrow 0$, and $\sigma_k \rightarrow \infty$, respectively, are given by:

$$(3.28) \quad \tilde{\mathcal{R}}_k^q(\sigma_k^0) = \lim_{\sigma_k \rightarrow 0} \tilde{\mathcal{R}}_k^q = \frac{\mathbf{r}_k \beta_k \rho_k}{\mathbf{p}_k \mathbf{q}_k \mathbf{r}_k}, \quad \text{and} \quad \tilde{\mathcal{R}}_k^q(\sigma_k^\infty) = \lim_{\sigma_k \rightarrow \infty} \tilde{\mathcal{R}}_k^q = \frac{\beta_k \rho_k}{\mathbf{p}_k \tilde{\mathbf{r}}_k},$$

where $k = c$ or i . The two equations given by (3.28), respectively, correspond to a maximum and minimum number of secondary infections generated when only infected are isolated. If none of the individuals is restricted or quarantined, in this case by setting $\alpha_k = \sigma_k = 0$, the that the corresponding reproduction number becomes

$$\mathcal{R} = \max\{\mathcal{R}_c, \mathcal{R}_i\}, \quad \text{where} \quad \mathcal{R}_k = \frac{\beta_k \rho_k}{(\rho_k + \mu)(\gamma_k + \delta_k + \mu)} \quad \text{and} \quad k = c \text{ or } i$$

Equation (3.27) and (3.28) implies that using quarantine (imperfect case) during an epidemic will not completely eradicate the disease in the population but will reduce the number of secondary infections and the disease complications, will decline accordingly. See Figure 6.

Symbol	Sensitivity coefficient (% change)					
	QRN		IRN		CQRN	
	$\tilde{\mathcal{R}}_i^q$	$\tilde{\mathcal{R}}_c^q$	${}_i\mathcal{I}_c^q$	${}_c\mathcal{I}_i^q$	\mathfrak{R}_i^c	\mathfrak{R}_c^i
Λ	-	-	$+4.5 \times 10^{-10}$	$+1.6 \times 10^{-7}$	-	-
β_i	+1.00000	-	+1.00000	-0.00113	+1.00000	-
β_c	-	+1.00000	-0.00118	+1.00000	-	+1.00000
ρ_i	+0.00932	-	+0.0565	-0.00014	-	-
ρ_c	-	+0.32106	-0.00827	+0.69968	-	-
ρ_{ic}	-	-	$+1.3 \times 10^{-10}$	$+1.1 \times 10^{-6}$	+0.78563	+0.78563
α_i	-0.03753	-	-0.05647	+0.00016	-	-
α_c	-	-0.32102	0.00827	-0.69964	-	-
α_{ic}	-	-	-1.3×10^{-10}	-1.1×10^{-6}	-0.78561	-0.78561
σ_i	-0.06626	-	-0.10778	+0.00030	-	-
σ_c	-	-0.03933	+0.00101	-0.08576	-	-
σ_{ic}	-	-	-1.5×10^{-10}	-1.3×10^{-6}	-0.89861	-0.89861
τ_i	+0.0120	-	+0.01527	-0.00004	-	-
τ_c	-	+0.01894	-0.00049	+0.04173	-	-
τ_{ic}	-	-	$+2.3 \times 10^{-11}$	$+2.0 \times 10^{-7}$	+0.13437	+0.13437
ϕ_i	-0.05116	-	-0.01527	+0.00004	-	-
ϕ_c	-	-0.42200	+0.00049	-0.04173	-	-
ϕ_{ic}	-	-	-2.3×10^{-11}	-2.0×10^{-7}	-0.13437	-0.13437
γ_i	-0.86599	-	-0.88922	+0.00252	-	-
γ_c	-	-0.52666	+0.01029	-0.87066	-	-
γ_{ic}	-	-	-1.7×10^{-11}	-1.5×10^{-7}	-10127	-10127
δ_i	-0.00297	-	-0.0029	+0.00167	-	-
δ_c	-	-0.0309	+0.00051	-0.04353	-	-
δ_{ic}	-	-	-1.7×10^{-14}	-1.5×10^{-10}	-0.00010	-0.00010
μ	-0.00011	-0.00006	-0.00006	-0.00011	-0.00003	-0.00003

Table 3

Sensitivity indices of the quarantine reproduction numbers, QRN & CQRN, and the invasion reproduction number (IRN). From the table, + means a positive relationship; - means a negative relationship; - means no relationship. Parameter values are $\Lambda = 0.0001$, $\beta_i = 0.9$, $\beta_c = 0.85$, $\rho_i = 0.3$, $\rho_c = 0.07$, $\rho_{ic} = 0.05$, $\tau_i = 0.02$, $\tau_c = 0.014$, $\tau_{ic} = 0.10$, $\alpha_i = 0.02$, $\alpha_c = 0.2$, $\alpha_{ic} = 0.5$, $\sigma_i = 0.04$, $\sigma_c = 0.02$, $\sigma_{ic} = 0.9$, $\delta_i = 0.001$, $\delta_c = 0.01$, $\delta_{ic} = 0.0001$, $\phi_i = 0.6$, $\phi_c = 0.92$, $\phi_{ic} = 0.7$, $\mu = 0.00001$, $\gamma_i = 0.3$, $\gamma_c = 0.2$, $\gamma_{ic} = 0.1$

3.5.3. Quarantine efficacy at the QRN . To know the critical rates corresponding to the imperfect quarantine, we solve for α_k and σ_k at $\tilde{\mathcal{R}}_k^q = 1$ to obtain α_k^* and σ_k^* , respectively; they are given by

$$(3.29) \quad \alpha_k^* = \frac{(\tilde{\mathcal{R}}_k^q(\alpha_k^0) - 1)\dot{\mathbf{p}}_k}{1 - \tilde{\mathcal{R}}_k^q(\alpha_k^\infty)} \quad \text{and} \quad \sigma_k^* = \frac{(\tilde{\mathcal{R}}_k^q(\sigma_k^0) - 1)\dot{\mathbf{q}}_k}{1 - \tilde{\mathcal{R}}_k^q(\sigma_k^\infty)}.$$

For further analysis, we use equation (2.1) after replacing the variable I_k by the expression of $\tilde{\mathcal{R}}_k^q$. The goal is to analyze how changes in α_k and σ_k affect the quarantine efficacy at the initial disease transmission. Thus,

$$\Omega_k = 1 - \omega_k \tilde{\mathcal{R}}_k^q,$$

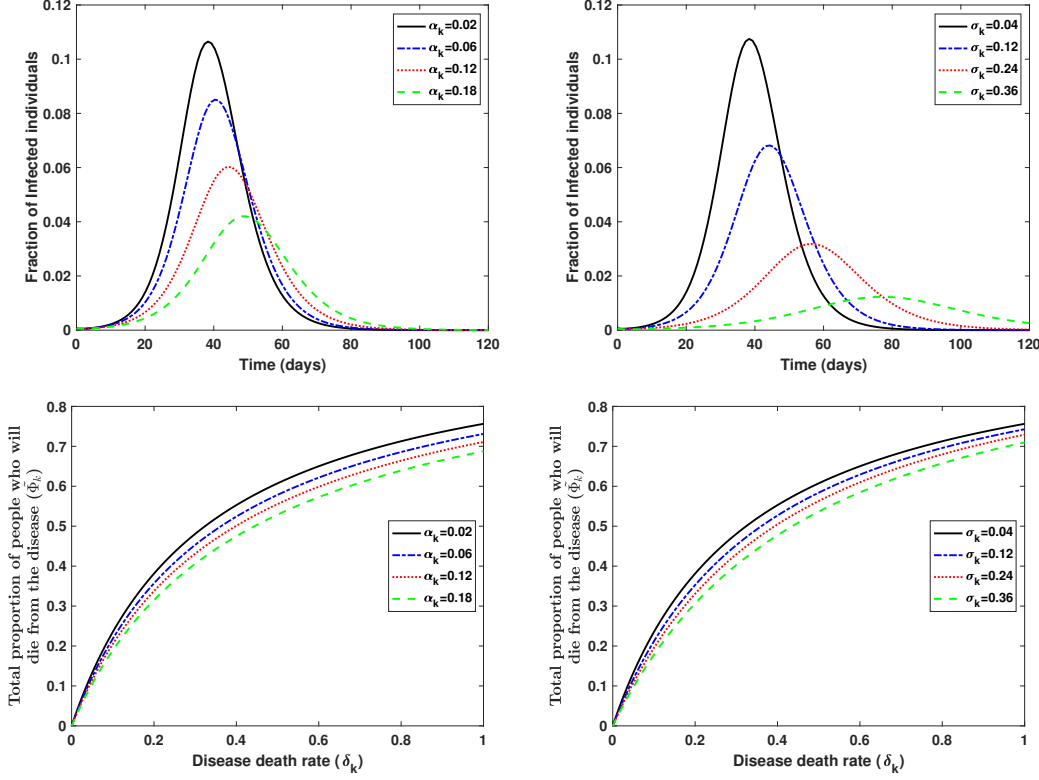


Figure 6. Numerical solutions of the fractions of infected individuals and the cumulative number of people who will die from the disease when α_k and σ_k change. Note in top and bottom left figures $\sigma_k = 0$. Further in top and bottom left figures $\alpha_k = 0$. The remaining used parameters are $\Lambda = 0.0001$, $\rho_k = 0.3$, $\tau_k = 0.06$, $\sigma_k = 0.04$, $\phi_k = 0.6$, $\mu = 0.0001$, $\gamma_k = 0.3$, $\beta_k = 0.9$, $\omega_k = 0.001$.

where $\omega_k \in (0, 1]$ (imperfect quarantine case). Differentiating Ω_k with respect to α_k and evaluating the result at $\omega_k = 1$, we obtain;

$$(3.30) \quad \frac{\partial \Omega_k}{\alpha_k} \Big|_{\omega_k=1} = \frac{\tilde{\mathcal{R}}_k^q - \tilde{\mathcal{R}}_k^q(\alpha_k^\infty)}{\mathbf{p}_c} > 0 \text{ positive impact if } \tilde{\mathcal{R}}_k^q > \tilde{\mathcal{R}}_k^q(\alpha_k^\infty)$$

The above-obtained equation means that when only exposed individuals are quarantined, the imperfect quarantine will have a positive impact provided that $\tilde{\mathcal{R}}_k^q > \tilde{\mathcal{R}}_k^q(\alpha_k^\infty)$. Similarly, differentiating Ω_k with respect to σ_k and evaluating the result at $\omega_k = 1$, we have

$$(3.31) \quad \frac{\partial \Omega_k}{\sigma_k} \Big|_{\omega_k=1} = (\tilde{\mathcal{R}}_k^q - \tilde{\mathcal{R}}_k^q(\sigma_k^\infty)) > 0 \text{ positive impact if } \tilde{\mathcal{R}}_k^q > \tilde{\mathcal{R}}_k^q(\sigma_k^\infty).$$

The numerical simulation of the quarantine reproduction number dependences on quarantine-related parameters together with the critical values estimates given in Equations (3.27) to (3.31) are visualized in Figure 7. Moreover, the figure compares the results of the perfect quarantine. With $\rho_k = 0.07$, $\alpha_k = \sigma_k = [0, 1]$, $\tau_k = 0.014$, $\gamma = 0.2$, $\phi_k = 0.92$, $\beta_k = 0.5$, $\delta_k = 0.001$, and $\mu = 0.0001$, the trajectories suggest that: the smaller the values of α_k and

σ_k , the higher the value of threshold $\tilde{\mathcal{R}}_k^q$ and vice versa. The crucial fact to note is that implementing perfect quarantine at the initial transmission could effectively eradicate the disease. These results are consistent with the findings on optimal and sub-optimal control of the SARS model [43].

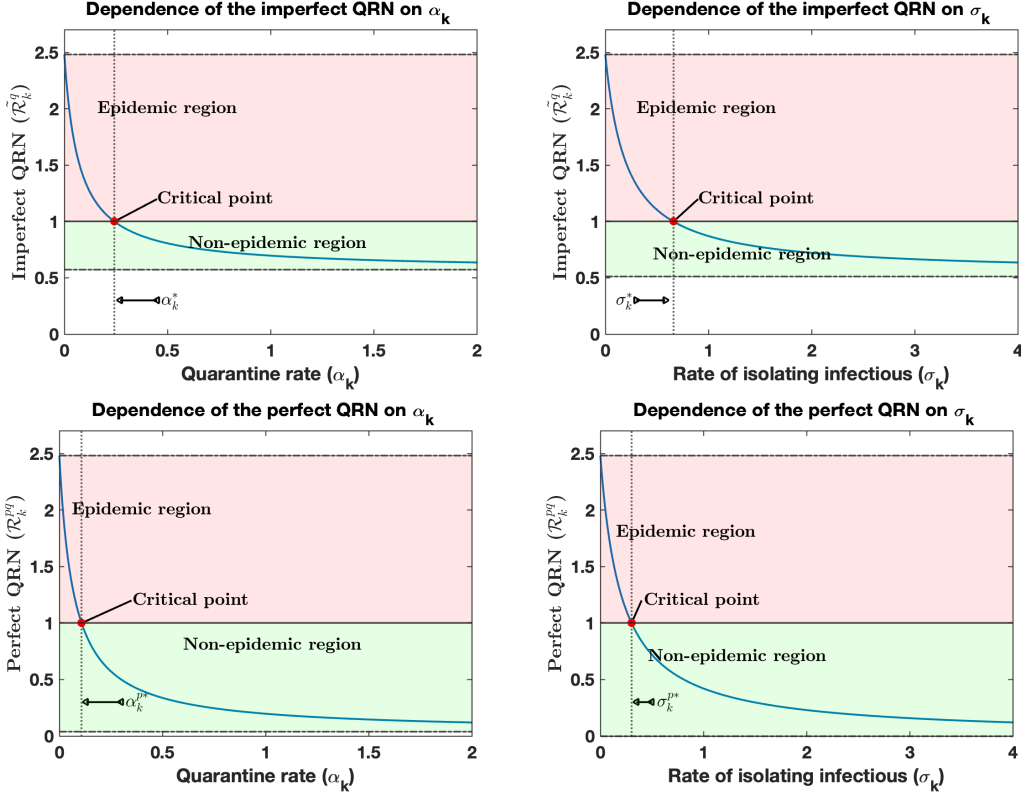


Figure 7. The dependence of the quarantine reproduction numbers (QRN) on the parameters related to the quarantine of exposed and infected, α_k and σ_k respectively. The parameters are $\beta_k = 0.5$, $\rho_k = 0.07$, $\phi_k = 0.92$, $\tau_k = 0.015$, $\mu = 0.0001$, $\gamma = 0.2$, $\delta_k = 0.001$.

Practicable questions, of course, are: what fractions of individuals should be restricted if the quarantine is imperfect (i.e., $0 < \Omega_k \leq 1$) with (i.) exposed only (ii.) infected only (iii.) both exposed and infected individuals? Let

$$\alpha_k^q = \frac{\alpha_k}{\mathbf{r}_k}, \quad \text{and,} \quad \sigma_k^q = \frac{\sigma_k}{\mathbf{r}_k},$$

respectively, give the fractions of quarantined individuals from the exposed and the infected classes. We substitute α_k and σ_k from (3.29) to obtain \mathbf{E}_k^{crit} and \mathbf{I}_k^{crit} , the critical levels of the exposed and infected individuals need to be restricted when the quarantine facility is imperfect. These levels, respectively, are given by

$$(3.32) \quad \mathbf{E}_k^{crit} = \frac{(\tilde{\mathcal{R}}_k^q(\alpha_k^0) - 1)\dot{\mathbf{p}}_k}{(1 - \tilde{\mathcal{R}}_k^q(\alpha_k^\infty))\mathbf{r}_k}, \quad \text{and,} \quad \mathbf{I}_k^{crit} = \frac{(\tilde{\mathcal{R}}_k^q(\sigma_k^0) - 1)\dot{\mathbf{q}}_k}{(1 - \tilde{\mathcal{R}}_k^q(\sigma_k^\infty))\mathbf{r}_k}.$$

In Figure 8, we estimate the fractions of quarantined individuals from the exposed and the infected classes and then determine the secondary cases for various α_k and σ_k . Moreover, we indicate the critical levels, \mathbf{E}_k^{crit} and \mathbf{I}_k^{crit} . The plots illustrate that applying quarantine (in the case of imperfect quarantine) will help to lower the secondary cases to less than unity if the rates of sending people to the quarantine are at least their critical values. In addition, the total number of people in the quarantine facility should not exceed its critical values (see region C in Figure 8. Lemma 3.11 summarizes these results.

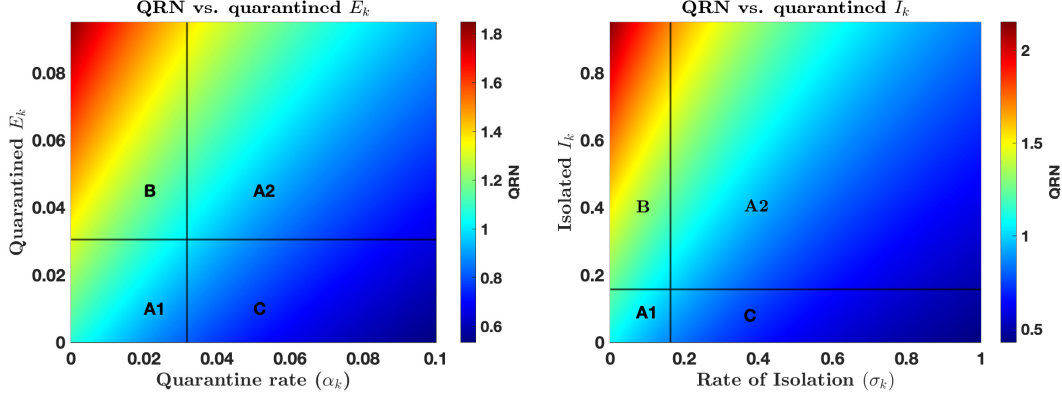


Figure 8. Relationship diagram showing how the parameters related to the quarantine (i.e., α_k and σ_k) and the proportions of individuals in the quarantine class influence the reproduction number. Here $\beta_k = 0.78$, $\rho_k = 0.09$, $\tau_k = 0.0135$, $\delta_k = 0.00001$, $\phi_k = 1.02$, $\mu = 0.009$, and $\gamma_k = 0.65$

Lemma 3.11. Given imperfect model (3.1),

1. when only exposed individuals are quarantined, the imperfect quarantine will have positive impact if and only if $\alpha_k \geq \alpha_k^*$, $\alpha_k^q \leq \mathbf{E}_k^{crit}$, and $\tilde{\mathcal{R}}_q^k > \tilde{\mathcal{R}}_q^k(\alpha_k^\infty) < 1$.
2. when only infected individuals are isolated, the imperfect quarantine will have positive impact if and only if $\sigma_k \geq \sigma_k^*$, $\sigma_k^q \leq \mathbf{I}_k^{crit}$, and $\tilde{\mathcal{R}}_q^k > \tilde{\mathcal{R}}_q^k(\sigma_k^\infty) < 1$;
3. when both exposed and infected individuals are restricted, we estimate the following results
 - (a) the overall rate of sending people in the quarantine should be $\max\{\alpha_k^*, \sigma_k^*\}$,
 - (b) the total number of people in the quarantine should be $\min\{\mathbf{E}_k^{crit}, \mathbf{I}_k^{crit}\}$.

Figure 9 gives some justification for the level of imperfection concerning the number of people in the quarantine and the potential input provided to control the disease. On top of that, it estimates the dependencies of quarantine time to the parameter ω_k . Lastly, the figure estimates the disease profile to the transmission rate and time to quarantine.

4. Conclusion and future work. We proposed the model with a single host population and multiple strains with co-infections. We started analyzing the model by assuming that only a single pathogen invaded the population. We examined the reproduction number and local stability using the next-generation approach. Employing the criterion introduced by Castillo-Chavez and his colleagues, we performed the global stability of the disease-free equilibrium.

Using the computer algebra systems, numerically, we solved the multi-strains model to predict the complex endemic equilibrium solution of the system. The (ξ_c^*, ξ_i^*) relationship in Figure 3 suggests that several endemic solutions are possible depending on the parameter

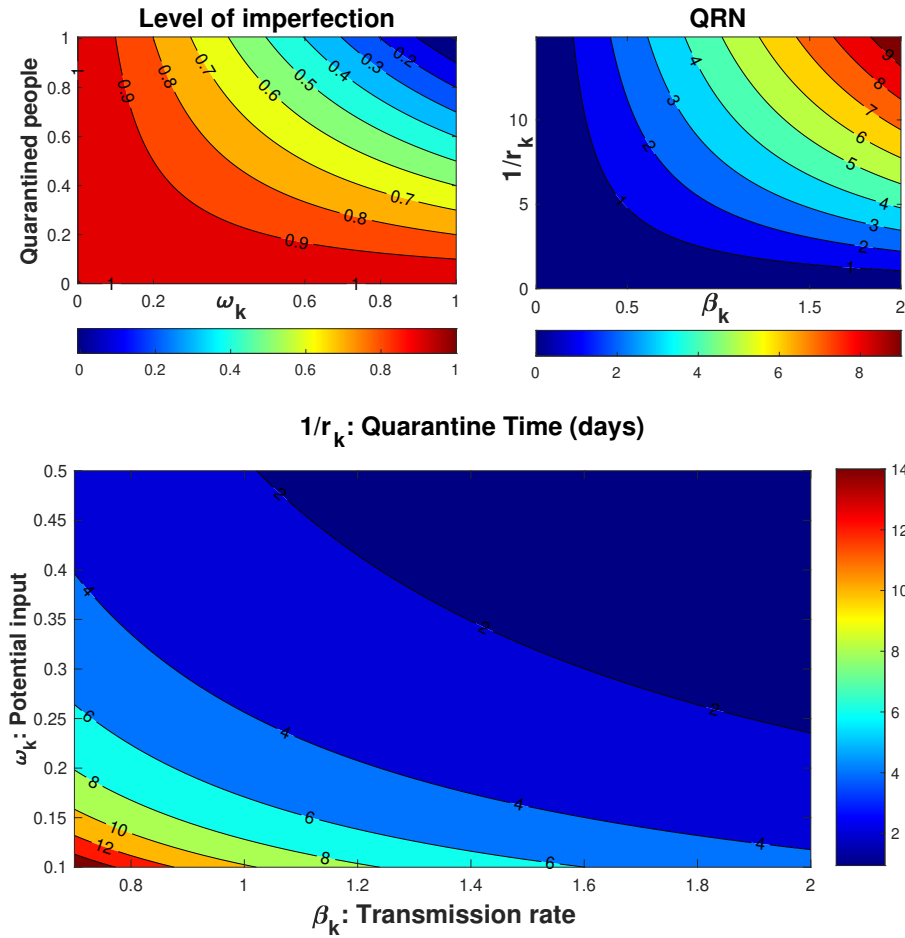


Figure 9. The *top left figure* estimates change in the level of imperfection, Ω_k , to the effort provided, ω_k , and the proportion number of individuals quarantined. The expected time in the quarantine concerning the potential parameter ω_k and the transmission rate β_k is given in the bottom figure. The *top right figure* gives the relationship between the transmission rate β_k , quarantine time, and infectiousness profile in terms of quarantine reproduction number, QRN. Parameters are taken as in *Figure 8*.

values. As in [Proposition 3.6](#), [Figure 5](#) shows that if $\tilde{\mathcal{R}}_k^q > 1$ (here $k = c$ or i) then the corresponding pathogen will dominate the system. Analysis in [Figure 4](#) tells how the cross-immunity parameters and the coexistence region are related. From a modeling point of view, this relationship notifies that; the smaller the value of the cross-immunity parameters, the smaller the fraction of the recovered population from one strain is susceptible to the second pathogen, consequently reducing the co-exposed individuals.

Moreover, our results provide a mathematical analysis of the impact of quarantine on the initial disease transmission and determine critical levels based on quarantine-related parameters. We note that the quarantine and isolation of exposed and infected individuals will reduce

the number of secondary cases consequently, reduce disease complications. See, for example, [Figure 6](#). Here we illustrated examples of disease complications: peak magnitude and people who will die from the disease. We found that as α_k and σ_k increase, the peak magnitude and the cumulative number of people who will die from the disease decline over time. However, the peak time and the final size could increase significantly.

Generally, proper application of rules and regulations (like waste management, accessibility to health care, and issues about hygiene) in the quarantine could result in less possibility of infection (less imperfection). See the top left illustration of [Figure 9](#). Additionally, from the bottom figure, as $\omega_k \rightarrow 0$, the quarantine duration is anticipated to be longer than when $\omega_k \rightarrow 1$, we can plausibly argue that the role played by the respective authority is essential to shorten the quarantine duration however, other parameters must be considered, for instance, the rates of transmission and recovery.

Here we made a few remarks. From a modeling point of view, the phenomenon of most co-infection diseases is still only partially understood. Principally, the intention of the proposed model was not to give a complete picture of the underlying behavior of competing or co-existing pathogens. Nevertheless, it provides the concept of various existing equilibria, the impact of quarantine as a control measure on the initial dynamic of the diseases, and cross-immune response. In addition, we solved the model (2.3) numerically, some parameter values when not available, so the assumed values were within a realistic range for illustrative purposes. Lastly, the linear equation (2.1) proved to work better in a model that used data [29]. However, the choice of function was reasonable to account for the decline of infections upon applying control measures, i.e., quarantine; one could use other types of declining functions.

Appendix A. Positivity and Boundedness.

A.1. Positivity of solutions of model 2.3.

Lemma A.1 (Positivity of solution). *Let*

$$(S(t), E_i(t), E_c(t), E_{ic}(t), I_i(t), I_c(t), I_{ic}(t), Q_i(t), Q_c(t), Q_{ic}(t), R_i(t), R_c(t), R_{ic}(t))$$

be the solution of the system (2.3). With initial conditions (2.4), the solution exists and remains non-negative for all $t \geq 0$.

Proof. Consider system (2.3), it follows from (2.4) that

$$\begin{aligned} \frac{dS}{dt} \Big|_{S=0} &= \Lambda > 0, \\ \frac{dE_i}{dt} \Big|_{E_i=0} &= \xi_i S + \eta_c R_c \xi_i \geq 0, \forall S, R_c \geq 0, \frac{dE_c}{dt} \Big|_{E_c=0} = \xi_c S + \eta_i R_i \xi_c, \forall S, R_i \geq 0, \\ \frac{dE_{ic}}{dt} \Big|_{E_{ic}=0} &= \xi_i I_c + \xi_c I_i \geq 0, \forall I_i, I_c \geq 0, \frac{dI_i}{dt} \Big|_{I_i=0} = \rho_i E_i + \tau_i Q_i \forall E_i, Q_i \geq 0, \\ \frac{dI_c}{dt} \Big|_{I_c=0} &= \rho_c E_c + \tau_c Q_c \forall E_c, Q_c \geq 0, \frac{dI_{ic}}{dt} \Big|_{I_{ic}=0} = \rho_{ic} E_{ic} + \tau_{ic} Q_{ic} \forall E_{ic}, Q_{ic} \geq 0, \\ \frac{dQ_i}{dt} \Big|_{Q_i=0} &= \alpha_i E_i + \sigma_i I_i \forall E_i, I_i \geq 0, \frac{dQ_c}{dt} \Big|_{Q_c=0} = \alpha_c E_c + \sigma_c I_c \forall E_c, I_c \geq 0, \\ \frac{dQ_{ic}}{dt} \Big|_{Q_{ic}=0} &= \alpha_{ic} E_{ic} + \sigma_{ic} I_{ic} \forall E_{ic}, I_{ic} \geq 0, \frac{dR_i}{dt} \Big|_{R_i=0} = \phi_i Q_i + \gamma_i I_i \forall Q_i, I_i \geq 0, \\ \frac{dR_c}{dt} \Big|_{R_c=0} &= \phi_c Q_c + \gamma_c I_c \forall Q_c, I_c \geq 0, \frac{dR_{ic}}{dt} \Big|_{R_{ic}=0} = \phi_{ic} Q_{ic} + \gamma_{ic} I_{ic} \forall Q_{ic}, I_{ic} \geq 0. \end{aligned}$$

We now prove that all solutions of (2.3) are non-negative as $t \rightarrow \infty$. From the first equation of the system, we have

$$\frac{dS}{dt} = \Lambda - (\xi_i + \xi_c + \mu)S \geq -(\xi_i + \xi_c + \mu)S,$$

after integration we obtain

$$S(t) = S(0)e^{-\int_0^t (\xi_i + \xi_c + \mu) ds} > 0 \text{ for all } t > 0.$$

It can be shown that $E_i(t) > 0, E_c(t) > 0, E_{ic}(t) > 0, I_i(t) > 0, I_c(t) > 0, I_{ic}(t) > 0, Q_i(t) > 0, Q_c(t) > 0, Q_{ic}(t) > 0, R_i(t) > 0, R_c(t) > 0, R_{ic}(t) > 0$ for all $t > 0$ analogously to $S(t)$. ■

A.2. Boundedness of solutions.

Lemma A.2 (Boundedness of solution). *The closed set*

$$\mathcal{C} = \left\{ (S, E_i, E_c, E_{ic}, I_i, I_c, I_{ic}, Q_i, Q_c, Q_{ic}, R_i, R_c, R_{ic}) \in \mathbb{R}_+^{13} : \right. \\ \left. S + E_i + E_c + E_{ic} + I_i + I_c + I_{ic} + Q_i + Q_c + Q_{ic} + R_i + R_c + R_{ic} \leq \frac{\Lambda}{\mu} \right\}$$

is positively-invariant for the model (2.3).

Proof. Adding all equations in the model (2.3) gives the rate of change in a total population over time:

$$(A.1) \quad N_T'(t) = \Lambda - \mu N_T - (\delta_c I_c + \delta_c Q_c + \delta_i I_i + \delta_i Q_i + \delta_{ic} I_{ic} + \delta_{ic} Q_{ic}).$$

From the equation (A.1), we have the condition

$$(A.2) \quad N_T'(t) \leq \Lambda - \mu N_T,$$

satisfied. Thus, the total population is bounded above, $N_T'(t) \leq 0$ whenever $N_T(t) \geq \Lambda/\mu$. From the equation (A.2), it is easy to see that

$$N_T(t) \leq \frac{\Lambda}{\mu} + \left(N_T(0) - \frac{\Lambda}{\mu} \right) e^{-\mu t}.$$

For any $t \geq 0$, the inequality above, gives

$$(A.3) \quad 0 < N_T(t) \leq \begin{cases} N_T(0), & \text{for } t = 0, \\ \Lambda/\mu, & \text{as } t \rightarrow \infty \end{cases}$$

Hence, the region \mathcal{C} is positive invariant and attracts all solutions in \mathbb{R}_+^{13} . ■

We have shown in Lemma A.2 that region \mathcal{C} is positive-invariant and attractive. Thus, it is sufficient to investigate the dynamics of (2.3) in \mathcal{C} , where the unique solution exists and continuously depends on the system data.

A.3. Non-negativity and boundness of solution of 3.1 .

Proposition A.3. *Let $(S(t), E_k(t), I_k(t), Q_k(t), R_k(t))$ be the solution of the system (3.1).*

1. *With initial conditions (2.4), the solution exists and remains non-negative for all $t \geq 0$.*
2. *The closed set*

$$\mathcal{C}_k = \left\{ (S, E_k, I_k, Q_k, R_k) \in \mathbb{R}_+^5 : S + E_k + I_k + Q_k + R_k \leq \frac{\Lambda}{\mu} \right\}$$

is positively-invariant for the model (3.1).

Proof. A similar way used to prove the positivity and boundedness of system (2.3) (i.e. subsection 2.3) can be used to show that the solutions of system (3.1) start in the set \mathcal{C}_k and remain there for all $t > 0$ and that \mathcal{C}_k attracts all solutions in \mathbb{R}_+^5 . Therefore, it is satisfactory to recognize the dynamics of (3.1) in \mathcal{C}_k . ■

Appendix B. Global Stability of the DFE-($\tilde{\mathbf{E}}^0$). We start by considering the closed set

$$\mathfrak{C} = \left\{ (S, E_i, E_c, I_i, I_c, Q_i, Q_c, R_i, R_c) \in \mathbb{R}_+^9 : \right. \\ \left. S + E_i + E_c + I_i + I_c + Q_i + Q_c + R_i + R_c \leq \frac{\Lambda}{\mu} \right\}$$

Lemma B.1. *The region \mathfrak{C} is positively-invariant for the model (3.11).*

Proof. In Lemma A.2, we have shown that the region \mathcal{C} is positively invariant and attractive. Since $\mathfrak{C} \subset \mathcal{C}$ by assumption, the region \mathfrak{C} is positively invariant and attractive. Thus, we recognize the coexistence model (3.11) to make biological sense in \mathfrak{C} . ■

Next, write system (3.11) in the form of equation 3.1 in [9] as follows: we denote a vector of uninfected individuals by $\mathbf{x} = (S, R_i, R_c)^T \in \mathbb{R}^3$ and that of infected individuals by $\mathbf{I} = (E_i, E_c, I_i, I_c, Q_i, Q_c)^T \in \mathbb{R}^6$ such that

$$(B.1) \quad \frac{d\mathbf{x}}{dt} = F(\mathbf{x}, \mathbf{I}), \quad \frac{d\mathbf{I}}{dt} = G(\mathbf{x}, \mathbf{I}).$$

We also denote the DFE, $\tilde{\mathbf{E}}^0 = (\mathbf{x}^*, 0, 0, 0, 0, 0)$ where \mathbf{x}^* define the DFE of system dx/dt . Moreover, we state the following conditions:

H1: For $F(\mathbf{x}, \mathbf{I})|_{\mathbf{x}^*}$, \mathbf{x}^* is globally asymptotically stable GAS,

H2: $G(\mathbf{x}, \mathbf{I}) = A\mathbf{I} - \hat{G}(\mathbf{x}, \mathbf{I})$, $\hat{G}(\mathbf{x}, \mathbf{I}) \geq 0$ for $(\mathbf{x}, \mathbf{I}) \in \mathfrak{C}$,

where $A = G(\mathbf{x}^*, 0)$ is an M -matrix. The following claim is true when the given two conditions hold for the system (3.11):

Theorem B.2. *The DFE $\tilde{\mathbf{E}}^0 = (\mathbf{x}^*, 0, 0, 0, 0, 0)$ of system (B.1), equivalent to (3.11) is globally asymptotically stable (GAS) if assumptions H1 and H2 holds and that $\max\{\mathcal{R}_c^q, \mathcal{R}_i^q\} < 1$ (LAS).*

Proof. Using next-generation approach we have shown in subsection 3.2.1 that

$$\max\{\tilde{\mathcal{R}}_c^q, \tilde{\mathcal{R}}_i^q\} < 1 \quad (LAS).$$

Let us now consider the prove for assumptions **H1** and **H2**. From (B.1), we have

$$F(\mathbf{x}, 0) = \begin{pmatrix} \Lambda - \mu S \\ 0 \\ 0 \end{pmatrix}, \quad A = \begin{pmatrix} -\mathbf{p}_1 & 0 & \beta_i & 0 & \beta_i & 0 \\ 0 & -\mathbf{p}_2 & 0 & \beta_c & 0 & \beta_c \\ \rho_i & 0 & -\mathbf{q}_1 & 0 & \tau_i & 0 \\ 0 & \rho_c & 0 & -\mathbf{q}_2 & 0 & \tau_c \\ \alpha_i & 0 & \sigma_i & 0 & -\mathbf{r}_1 & 0 \\ 0 & \alpha_c & 0 & \sigma_c & 0 & -\mathbf{r}_2 \end{pmatrix},$$

and,

$$\hat{G}(\mathbf{x}, \mathbf{I}) = \begin{pmatrix} \beta_i I_i (1 - \frac{S}{N}) + \beta_i Q_i (1 - \frac{\Omega_i S}{N}) \\ \beta_c I_c (1 - \frac{S}{N}) + \beta_c Q_c (1 - \frac{\Omega_c S}{N}) \\ 0 \\ 0 \\ 0 \\ 0 \end{pmatrix}.$$

It follows that $\Omega_i, \Omega_c \in (0, 1]$, and $0 \leq \Omega_i S, \Omega_c S \leq S \leq N$ then $\hat{G}(\mathbf{x}, \mathbf{I}) \geq 0$ (**H2** holds). Moreover,

$$\lim_{t \rightarrow \infty} F(\mathbf{x}(t), \mathbf{I}(t))|_{\mathbf{x}^*} = \lim_{t \rightarrow \infty} F(\mathbf{x}(t), 0) = (\frac{\Lambda}{\mu}, 0, 0) = \mathbf{x}^*, \quad \mathbf{H1} \text{ holds.} \quad \blacksquare$$

Appendix C. Invasion reproduction number (IRN). The infectious classes E_i, I_i , & Q_i are linearized when strain- c is resident. The vector of new infections \mathcal{F} and outflow vector \mathcal{V} are given by

$$(C.1) \quad \mathcal{F} = \begin{pmatrix} \xi_i S + \eta_c R_c \xi_i \\ 0 \\ 0 \end{pmatrix} \quad \text{and} \quad \mathcal{V} = \begin{pmatrix} \mathbf{p}_i E_i \\ \mathbf{q}_i I_i - \rho_i E_i + \tau_i Q_i \\ \mathbf{r}_i Q_i - \alpha_i E_i - \sigma_i I_i \end{pmatrix}$$

We take the derivatives of \mathcal{F} and \mathcal{V} and evaluate at (3.13) to obtain matrices, namely:

$$(C.2) \quad F = \begin{pmatrix} 0 & \tilde{S}_c^* \beta_i + \tilde{R}_c^* \beta_i \eta_c & 0 \\ 0 & 0 & 0 \\ 0 & 0 & 0 \end{pmatrix} \quad \text{and} \quad V = \begin{pmatrix} \mathbf{p}_i & 0 & 0 \\ -\rho_i & \mathbf{q}_i & -\tau_i \\ -\alpha_i & -\sigma_i & \mathbf{r}_i \end{pmatrix}$$

The strain- i invasion reproduction number is then defined as ${}_i \tilde{\mathcal{R}}_c^q = \rho(FV^{-1})$.

Acknowledgments. A.D.F. thanks the German Academic Exchange Service for the doctoral studies financial supports.

REFERENCES

- [1] M. A. ACUÑA-ZEGARRA, M. NÚÑEZ-LÓPEZ, A. COMAS-GARCÍA, M. SANTANA-CIBRIAN, AND J. X. VELASCO-HERNÁNDEZ, *Co-circulation of sars-cov-2 and influenza under vaccination scenarios*, medRxiv, (2021), pp. 2020–12, <https://www.medrxiv.org/content/10.1101/2020.12.29.20248953v2>.

- [2] P. AGARWAL, J. J. NIETO, M. RUZHANSKY, AND D. F. TORRES, *Analysis of infectious disease problems (Covid-19) and their global impact*, Springer, 2021.
- [3] M. ALI, S. T. H. SHAH, M. IMRAN, AND A. KHAN, *The role of asymptomatic class, quarantine and isolation in the transmission of covid-19*, *Journal of biological dynamics*, 14 (2020), pp. 389–408, <https://doi.org/10.1080/17513758.2020.1773000>.
- [4] N. M. ALMAZÁN, A. RAHBAR, M. CARLSSON, T. HOFFMAN, L. KOLSTAD, B. RÖNNBERG, M. R. PANTALONE, I. L. FUCHS, A. NAUCLÉR, M. OHLIN, ET AL., *Influenza a h1n1-mediated pre-existing immunity to sars-cov-2 predicts covid-19 outbreak dynamics*, *medRxiv*, (2021), pp. 2021–12, <https://doi.org/10.1101/2021.12.23.21268321>.
- [5] B. ALOSAIMI, A. NAEEM, M. E. HAMED, H. S. ALKADI, T. ALANAZI, S. S. AL REHILY, A. Z. ALMUTAIRI, AND A. ZAFAR, *Influenza co-infection associated with severity and mortality in covid-19 patients*, *Virology journal*, 18 (2021), pp. 1–9, <https://www.ncbi.nlm.nih.gov/pmc/articles/PMC8200793/>.
- [6] M. S. ARONNA, R. GUGLIELMI, AND L. M. MOSCHEN, *A model for covid-19 with isolation, quarantine and testing as control measures*, *Epidemics*, 34 (2021), p. 100437, <https://doi.org/10.1016/j.epidem.2021.100437>.
- [7] P. ASHCROFT, S. LEHTINEN, D. C. ANGST, N. LOW, AND S. BONHOEFFER, *Quantifying the impact of quarantine duration on covid-19 transmission*, *Elife*, 10 (2021), p. e63704, <https://doi.org/10.7554/eLife.63704>.
- [8] S. BHOWMICK, I. M. SOKOLOV, AND H. H. LENTZ, *Decoding the double trouble: A mathematical modelling of co-infection dynamics of sars-cov-2 and influenza-like illness*, *Biosystems*, (2023), p. 104827, <https://pubmed.ncbi.nlm.nih.gov/36626949/>.
- [9] C. CASTILLO-CHAVEZ, *On the computation of r . and its role on global stability carlos castillo-chavez*, zhilan feng, and wenzhang huang*, *Mathematical approaches for emerging and reemerging infectious diseases: an introduction*, 1 (2002), p. 229, https://web.archive.org/web/20040510231721id_/http://0-math.la.asu.edu.csulib.ctstateu.edu:80/~chavez/2002/JB276.pdf.
- [10] C. CASTILLO-CHAVEZ, H. W. HETHCOTE, V. ANDREASEN, S. A. LEVIN, AND W. M. LIU, *Epidemiological models with age structure, proportionate mixing, and cross-immunity*, *Journal of mathematical biology*, 27 (1989), pp. 233–258, <https://link.springer.com/article/10.1007/BF00275810>.
- [11] C. CASTILLO-CHAVEZ AND B. SONG, *Dynamical models of tuberculosis and their applications*, *Math. Biosci. Eng.*, 1 (2004), pp. 361–404, <https://doi.org/10.3934/mbe.2004.1.361>.
- [12] Z. CHLADNÁ, J. KOPFOVÁ, D. RACHINSKII, AND P. ŠTEPÁNEK, *Effect of quarantine strategies in a compartmental model with asymptomatic groups*, *Journal of Dynamics and Differential Equations*, (2021), pp. 1–24, <https://www.ncbi.nlm.nih.gov/pmc/articles/PMC8385487/>.
- [13] A. A. CRUZ, *Global surveillance, prevention and control of chronic respiratory diseases: a comprehensive approach*, World Health Organization, 2007, <https://apps.who.int/iris/bitstream/handle/10665/43776/9789241563468eng.pdf?sequence=1>.
- [14] M. DADASHI, S. KHALEGHNEJAD, P. ABEDI ELKHICHI, M. GOUDARZI, H. GOUDARZI, A. TAGHAVI, M. VAEZJALALI, AND B. HAJIKHANI, *Covid-19 and influenza co-infection: a systematic review and meta-analysis*, *Frontiers in medicine*, 8 (2021), p. 681469, <https://www.ncbi.nlm.nih.gov/pmc/articles/PMC8267808/>.
- [15] S. E. EIKENBERRY, M. MANCUSO, E. IBOI, T. PHAN, K. EIKENBERRY, Y. KUANG, E. KOSTELICH, AND A. B. GUMEL, *To mask or not to mask: Modeling the potential for face mask use by the general public to curtail the covid-19 pandemic*, *Infectious disease modelling*, 5 (2020), pp. 293–308, <https://www.sciencedirect.com/science/article/pii/S2468042720300117>.
- [16] A. D. FOME, H. RWEZAURA, M. L. DIAGNE, S. COLLINSON, AND J. M. TCHUENCHE, *A deterministic susceptible-infected-recovered model for studying the impact of media on epidemic dynamics*, *Healthcare Analytics*, (2023), p. 100189, <https://doi.org/10.1016/j.health.2023.100189>.
- [17] M. FUDOLIG AND R. HOWARD, *The local stability of a modified multi-strain sir model for emerging viral strains*, *PloS one*, 15 (2020), p. e0243408, <https://journals.plos.org/plosone/article?id=10.1371/journal.pone.0243408>.
- [18] D. M. HAMBY, *A review of techniques for parameter sensitivity analysis of environmental models*, *Environmental monitoring and assessment*, 32 (1994), pp. 135–154, <https://doi.org/10.1007/BF00547132>.
- [19] H. W. HETHCOTE, *Three basic epidemiological models*, *Applied mathematical ecology*, (1989), pp. 119–

- 144, <https://link.springer.com/chapter/10.1007/978-3-642-61317-35>.
- [20] N. JEBRIL, *World health organization declared a pandemic public health menace: a systematic review of the coronavirus disease 2019 "covid-19"*, Available at SSRN 3566298, (2020), <https://papers.ssrn.com/sol3/papers.cfm?abstractid=3566298>.
- [21] O. KHYAR AND K. ALLALI, *Global dynamics of a multi-strain seir epidemic model with general incidence rates: application to covid-19 pandemic*, *Nonlinear dynamics*, 102 (2020), pp. 489–509, <https://www.ncbi.nlm.nih.gov/pmc/articles/PMC7478444/>.
- [22] M. E. KITLER, P. GAVINIO, AND D. LAVANCHY, *Influenza and the work of the world health organization*, *Vaccine*, 20 (2002), pp. S5–S14, [https://doi.org/10.1016/S0264-410X\(02\)00121-4](https://doi.org/10.1016/S0264-410X(02)00121-4).
- [23] V. M. KONALA, S. ADAPA, V. GAYAM, S. NARAMALA, S. R. DAGGUBATI, C. B. KAMMARI, AND A. CHENNA, *Co-infection with influenza a and covid-19*, *European journal of case reports in internal medicine*, 7 (2020), <https://www.ejcrim.com/index.php/EJCRIM/article/view/1656>.
- [24] C.-C. LAI, C.-Y. WANG, AND P.-R. HSUEH, *Co-infections among patients with covid-19: The need for combination therapy with non-anti-sars-cov-2 agents?*, *Journal of Microbiology, Immunology and Infection*, 53 (2020), pp. 505–512, <https://doi.org/10.1016/j.jmii.2020.05.013>.
- [25] L. LANSBURY, B. LIM, V. BASKARAN, AND W. S. LIM, *Co-infections in people with covid-19: a systematic review and meta-analysis*, *Journal of Infection*, 81 (2020), pp. 266–275, <https://doi.org/10.1016/j.jinf.2020.05.046>.
- [26] T. LAZEBNIK AND S. BUNIMOVICH-MENDRAZITSKY, *Generic approach for mathematical model of multi-strain pandemics*, *PloS one*, 17 (2022), p. e0260683, <https://doi.org/10.1371/journal.pone.0260683>.
- [27] D. MARCINIUK, T. FERKOL, A. NANA, M. M. DE OCA, K. RABE, N. BILLO, AND H. ZAR, *Respiratory diseases in the world. realities of today–opportunities for tomorrow*, *African Journal of Respiratory Medicine* Vol, 9 (2014), <https://www.africanjournalofrespiratorymedicine.com/articles/AJRM%20Mar%2014%20pp%204-13.pdf>.
- [28] M. MARTCHEVA, *An introduction to mathematical epidemiology*, vol. 61, Springer, 2015, <https://link.springer.com/book/10.1007/978-1-4899-7612-3>.
- [29] L. MITCHELL AND J. V. ROSS, *A data-driven model for influenza transmission incorporating media effects*, *Royal Society open science*, 3 (2016), p. 160481, <https://doi.org/10.1098/rsos.160481>.
- [30] J. D. MURRAY, *Mathematical biology: I. An introduction. Interdisciplinary applied mathematics*, vol. 17, *Mathematical Biology*, Springer, 2002.
- [31] M. NUÑO, Z. FENG, M. MARTCHEVA, AND C. CASTILLO-CHAVEZ, *Dynamics of two-strain influenza with isolation and partial cross-immunity*, *SIAM Journal on Applied Mathematics*, 65 (2005), pp. 964–982, <https://doi.org/10.1137/S003613990343882X>.
- [32] M. M. OJO, T. O. BENSON, O. J. PETER, AND E. F. D. GOUFO, *Nonlinear optimal control strategies for a mathematical model of covid-19 and influenza co-infection*, *Physica A: Statistical Mechanics and its Applications*, 607 (2022), p. 128173, <https://doi.org/10.1016/j.physa.2022.128173>.
- [33] W. H. ORGANIZATION ET AL., *Infection prevention and control of epidemic-and pandemic-prone acute respiratory infections in health care*, World Health Organization, 2014, <https://apps.who.int/iris/bitstream/handle/10665/112656/97892?sequence=1>.
- [34] W. H. ORGANIZATION ET AL., *Considerations for quarantine of contacts of covid-19 cases: interim guidance, 19 august 2020*, tech. report, World Health Organization, 2020, <https://apps.who.int/iris/bitstream/handle/10665/333901/WHO-2019-nCoV-IHRQuarantine-2020.3-eng.pdf>.
- [35] A. G. PÉREZ AND D. A. OLUYORI, *A model for covid-19 and bacterial pneumonia coinfection with community-and hospital-acquired infections*, arXiv preprint arXiv:2207.13265, (2022), <https://doi.org/10.48550/arXiv.2207.13265>.
- [36] L. PINKY AND H. M. DOBROVOLNY, *Sars-cov-2 coinfections: Could influenza and the common cold be beneficial?*, *Journal of Medical Virology*, 92 (2020), pp. 2623–2630, <https://www.ncbi.nlm.nih.gov/pmc/articles/PMC7300957/>.
- [37] M. SAMSUZZOHA, M. SINGH, AND D. LUCY, *Uncertainty and sensitivity analysis of the basic reproduction number of a vaccinated epidemic model of influenza*, *Applied Mathematical Modelling*, 37 (2013), pp. 903–915, <https://doi.org/10.1016/j.apm.2012.03.029>.
- [38] B. SINGH, P. KAUR, R.-J. REID, F. SHAMOON, AND M. BIKKINA, *Covid-19 and influenza co-infection: report of three cases*, *Cureus*, 12 (2020), <https://www.ncbi.nlm.nih.gov/pmc/articles/PMC7437098/>.
- [39] B. SONI AND S. SINGH, *Covid-19 co-infection mathematical model as guided through signaling structural*

- framework*, Computational and Structural Biotechnology Journal, 19 (2021), pp. 1672–1683, <https://doi.org/10.1016/j.csbj.2021.03.028>.
- [40] I. STEFANSKA, M. ROMANOWSKA, S. DONEVSKI, D. GAWRYLUK, AND L. B. BRYDAK, *Co-infections with influenza and other respiratory viruses*, in Respiratory Regulation-The Molecular Approach, Springer, 2013, pp. 291–301, <https://www.ncbi.nlm.nih.gov/pmc/articles/PMC7120114/>.
- [41] B. TANG, N. L. BRAGAZZI, Q. LI, S. TANG, Y. XIAO, AND J. WU, *An updated estimation of the risk of transmission of the novel coronavirus (2019-ncov)*, Infectious disease modelling, 5 (2020), pp. 248–255, <https://doi.org/10.1016/j.idm.2020.02.001>.
- [42] P. VAN DEN DRIESSCHE AND J. WATMOUGH, *Reproduction numbers and sub-threshold endemic equilibria for compartmental models of disease transmission*, Mathematical biosciences, 180 (2002), pp. 29–48, [https://doi.org/10.1016/S0025-5564\(02\)00108-6](https://doi.org/10.1016/S0025-5564(02)00108-6).
- [43] X. YAN AND Y. ZOU, *Optimal and sub-optimal quarantine and isolation control in sars epidemics*, Mathematical and computer modelling, 47 (2008), pp. 235–245, <https://doi.org/10.1016/j.mcm.2007.04.003>.
- [44] Y. ZHOU, B. SONG, AND Z. MA, *The global stability analysis for an sis model with age and infection age structures*, in Mathematical approaches for emerging and reemerging infectious diseases: models, methods, and theory, Springer, 2002, pp. 313–335, <https://link.springer.com/content/pdf/10.1007/978-1-4613-0065-6.pdf>.
- [45] X. ZHU, Y. GE, T. WU, K. ZHAO, Y. CHEN, B. WU, F. ZHU, B. ZHU, AND L. CUI, *Co-infection with respiratory pathogens among covid-2019 cases*, Virus research, 285 (2020), p. 198005, <https://doi.org/10.1016/j.virusres.2020.198005>.